Predicting the spatial and temporal dynamics of species interactions in *Fagus sylvatica* and *Pinus sylvestris* forests across Europe

D.I. Forrester[a,b,*], Ch. Ammer[c], P.J. Annighöfer[c], A. Avdagic[d], I. Barbeito[e], K. Bielak[f], G. Brazaitis[g], L. Coll[h], M. del Río[i,j], L. Drössler[k], M. Heym[l], V. Hurt[m], M. Löf[k], B. Matović[n], F. Meloni[o], J. den Ouden[p], M. Pach[q], M.G. Pereira[r], Q. Ponette[s], H. Pretzsch[l], J. Skrzyszewski[q], D. Stojanović[n], M. Svoboda[t], R. Ruiz-Peinado[i,j], G. Vacchiano[o,u], K. Verheyen[v], T. Zlatanov[w], A. Bravo-Oviedo[i,j]

[a] Swiss Federal Institute for Forest, Snow and Landscape Research WSL, Birmensdorf, Switzerland
[b] Chair of Silviculture, Albert-Ludwigs-Universität Freiburg, Germany
[c] Silviculture and Forest Ecology of the Temperate Zones, Georg-August-Universität Göttingen, Germany
[d] Department of Forest Management and Urban Greenery, Faculty of Forestry, University Sarajevo, Bosnia and Herzegovina
[e] Laboratoire d'Etude des Ressources Forêt Bois (LERFoB), INRA Centre of Nancy, Champenoux, France
[f] Department of Silviculture, Warsaw University of Life Sciences, Poland
[g] Institute of Forest Biology and Silviculture, Aleksandras, Stulginskis University, Kaunas, Lithuania
[h] Department of Agriculture and Forest Engineering – Forest Sciences Centre of Catalonia (CTFC), University of Lleida, Spain
[i] Department of Silviculture and Forest Management, INIA, Forest Research Centre INIA-CIFOR Forest Research Centre, Crta. La Coruña km 7,5, 28040 Madrid, Spain
[j] Sustainable Forest Management Research Institute, University of Valladolid & INIA, Spain
[k] Southern Swedish Forest Research Centre, Swedish University of Agricultural Sciences, Alnarp, Sweden
[l] Chair for Forest Growth and Yield Science, Technische Universität München, Germany
[m] Department of Silviculture, Mendel University, Brno, Czech Republic
[n] Institute of Lowland Forestry and Environment, University of Novi Sad, Novi Sad, Serbia
[o] Department of Agricultural, Forest and Food Sciences, DISAFA, University of Turin, Turin, Italy
[p] Forest Ecology and Forest Management Group, Wageningen University & Research, Wageningen, The Netherlands
[q] Department of Silviculture, Institute of Forest Ecology and Silviculture, University of Agriculture, Krakow, Poland
[r] Centro de Investigação e de Tecnologias Agro-Ambientais e Biológicas, CITAB, Universidade de Trás-os-Montes e Alto Douro, UTAD, Quinta de Prados, 5000-801 Vila Real, Portugal
[s] Universite Catholique de Louvain, Faculty of Bioscience Engineering & Earth and Life Institute, Louvain-la-Neuve, Belgium
[t] Faculty of Forestry and Wood Sciences, Czech University of Life Sciences, Prague, Czech Republic
[u] currently at: European Commission, Joint Research Centre, Directorate D – Sustainable Resources – Bio-Economy Unit, via E. Fermi 2749 – TP261, I-21027 Ispra, VA, Italy
[v] Forest & Nature Lab, Ghent University, Melle-Gontrode, Belgium
[w] Department of Silviculture, Forest Research Institute, Sofia, Bulgaria

ARTICLE INFO

ABSTRACT

The productivity and functioning of mixed-species forests often differs from that of monocultures. However, the magnitude and direction of these differences are difficult to predict because species interactions can be modified by many potentially interacting climatic and edaphic conditions, stand structure and previous management. Process-based forest growth models could potentially be used to disentangle the effects of these factors and thereby improve our understanding of mixed forest functioning while facilitating their design and silvicultural management. However, to date, the predicted mixing effects of forest growth models have not been compared with measured mixing effects. In this study, 26 sites across Europe, each containing a mixture and monocultures of *Fagus sylvatica* and *Pinus sylvestris*, were used to calculate mixing effects on growth and yield and compare them with the mixing effects predicted by the forest growth model 3-PG$_{mix}$. The climate and edaphic conditions, stand structures and ages varied greatly between sites. The model performed well when predicting the stem mass and total mass (and mixing effects on these components), with model efficiency that was usually > 0.7. The model efficiency was lower for growth or smaller components such as foliage mass and root mass. The model was also used to predict how mixing effects would change along gradients in precipitation, temperature, potential available soil water, age, thinning intensity and soil fertility. The predicted patterns were consistent with

* Corresponding author at: Swiss Federal Institute of Forest, Snow and Landscape Research WSL, Zürcherstrasse 111, 8903 Birmensdorf, Switzerland.
E-mail address: david.forrester@wsl.ch (D.I. Forrester).

measurements of mixing effects from published studies. The 3-PG model is a widely used management tool for monospecific stands and this study shows that 3-PG$_{mix}$ can be used to examine the dynamics of mixed-species stands and determine how they may need to be managed.

1. Introduction

Forest productivity, functioning and stability can differ greatly between mixed-species forests and monocultures. The magnitude and direction of these differences are often uncertain because they are influenced by many potentially interacting factors, including species traits, climatic and edaphic conditions, stand structure and previous management (Forrester, 2014; Bauhus et al., 2017a). Forest growth models are frequently used to predict and disentangle the effects of these factors, which are often occurring and changing simultaneously. When empirical datasets cover an appropriate range in these factors, empirical analyses or models can be developed to predict the growth and yield (Mette et al., 2009; Huber et al., 2014; Pretzsch et al., 2015a). However, usually these data do not exist, or the questions being asked are relating to causality, such as *why* a response occurred and not only *how* the forest responded. In this case, process-based models are useful.

Despite the potential of process-based models to predict mixing effects in forests, a recent review found no models that have been tested by comparing the predicted mixing effects with measured mixing effects (Pretzsch et al., 2015b). Therefore, there is an urgent need to test the ability of forest growth models to predict mixing effects. In this study, mixing effects are quantified using the relative productivity (RP); in the form of Eq. (1) for the whole mixed stand or Eq. (2) for each individual species (Forrester and Pretzsch, 2015).

$$RP_{total\ stand} = \frac{p_{1,2}}{m_1 p_1 + m_2 p_2} \tag{1}$$

$$RP_{species\ 1} = \frac{p_{1,(2)}}{m_1 p_1} \tag{2}$$

The $p_{1,2}$ is the growth or yield of the whole mixture and $p_{1,(2)}$ is the growth or yield of species 1 in a mixture with species 2. The p_1 and p_2 are the growth or yield of species 1 and species 2 in their respective monocultures. The m_1 and m_2 are the mixing proportions calculated from the basal area of each species. When RP = 1 the growth or yield of the mixtures is exactly as expected based on the monocultures (i.e. an additive effect), indicating no complementarity effect. RP > 1 or RP < 1 indicate overyielding and underyielding effects, respectively, where overyielding occurs when mixtures produce more than the weighted mean of monocultures, and underyielding occurs when mixtures produce less than the weighted mean of monocultures.

Confidence in the predictions of mixing effects cannot be expected until a given model has been carefully validated. This is more important when modelling mixed-species forests than it is when modelling

Table 1

Major processes or species interactions that can influence the growth of mixtures compared with monocultures, modified from Forrester and Bauhus (2016), and whether they can be simulated using the 3-PG$_{mix}$ model. The "Manual" label in the middle column indicates that the process can be simulated by inputting a time series of values for the relevant parameter to reflect its temporal change, based on the user's knowledge of that process, e.g., if rates of nitrogen fixation change, then the fertility parameters may need to change through time.

Name of process or pattern	Presence in 3-PG$_{mix}$	Notes
Nutrient-related		
Symbiotic nitrogen fixation	Manual	Can be simulated manually by changing the fertility rating when the timing and
Nutrient cycling	Manual	magnitude of the change is known. Or by linking 3-PG$_{mix}$ with a nutrient model
Chemical, spatial or temporal stratification	Manual	(e.g., Xenakis et al., 2008)
Nutrient mineralization	Manual	
Canopy nitrogen retention	Manual	
Light-related		
Space occupation – canopy stratification	Yes	
Space occupation – complementary crown shapes and architectures	Yes	Shapes are limited to cones, ellipsoids, half-ellipsoids and boxes
Space occupation – intra-specific variability in crown architecture and size, or influence of inter-specific competition on intra-specific variability	Yes	Variability in crown architecture via parameters for height, live-crown length and crown diameter equations
Physiological differences	Yes	e.g. light-use efficiency can be reduced relative to the species potential (α_{Cx}) in response to mixing effects on within canopy vapour pressure deficit, soil moisture and soil fertility.
Phenology and inter-specific effects on these	Manual	Simulated by changing the parameters determining leaf fall and bud break
Water-related		
Hydraulic redistribution	Manual	By using the irrigation silvicultural treatment or changing the available soil water during the simulation
Shared mycorrhizal networks	No	
Canopy interception	Yes	
Transpiration and water-use efficiency	Yes	
Litter layer as a sponge or barrier	Manual	By using the irrigation silvicultural treatment or changing the available soil water during the simulation
Isohydric vs. Anisohydric	Yes	e.g. via the parameter defining stomatal responses to vapour pressure deficit (k_D)
Inter-and intra-specific differences in phenology	Manual	Simulated by changing the parameters determining leaf fall and bud break
Modified within-stand environmental conditions	Yes	
Biotic		
Insect herbivory and leaf pathogens	Manual	e.g. by using the pruning silvicultural treatment or changing the foliage biomass
Other		
Carbon partitioning	Yes	Mixing effects on partitioning to roots relative to aboveground growth occur via changes in soil fertility, vapour pressure deficit within the canopy and soil moisture, while partitioning between stems and foliage is related to mixing effects on tree size (larger trees partition a lower proportion of NPP to foliage)

monocultures because in a mixture, if one species is modelled incorrectly, the predicted competition that species has on all the other species will be incorrectly modelled and any associated bias will build up as the simulation progresses, leading to unrealistic stand dynamics.

There are at least three criteria that should be used when selecting a model to simulate the dynamics of mixed-species forests. Firstly, the model should simulate the processes and interactions that are likely to be important in the target mixed forest. Some of these are listed in Table 1. While many tree level models can simulate most of these processes (e.g., Maestra or Maestro; Medlyn, 2004), they often require extensive data for parameterization and operate at high temporal and spatial resolutions, which results in high computational demands. Calculations at high resolutions (e.g. leaves and hours) can also result in errors that are propagated when upscaling, and high resolutions are not necessary when the desired outputs are at lower temporal (months or years) or spatial (stands) resolutions, such as those often required by forest managers. Furthermore, many important processes and interactions shown in Table 1 can be calculated at the cohort and stand levels (not only at the tree or leaf levels) (Pretzsch et al., 2015b). Therefore, stand level models have been used to reduce computation demands and to avoid the propagation of bias associated with upscaling (e.g., Härkönen et al., 2010; Forrester and Tang, 2016).

The second criterion is that all processes (e.g., equations or sub-models) that the model includes should have been evaluated by comparing predictions against empirical data (Grimm, 1999; Weiskittel et al., 2010), preferably for many different forest types and species. That is, it is easy to achieve a very good fit to observed growth and yield data for the wrong physiological reasons (Sands, 2004). Good

predictions of growth and yield do not reliably indicate whether the other calculations (light, water balance, carbon partitioning, nutrient cycling) are accurate or therefore whether the model is reliable.

The third criterion is that species-specific parameters must not change with species interactions. Species interactions can change the resource availability and within-stand climatic conditions and thereby the physiological performance of a given species, but they cannot change the basic physiology of that species; in other words, the species cannot change into a different species. Therefore, it should be possible to use a single parameter set for a given species (or provenance or clone) to simulate its response to competition, climatic and edaphic factors. For example, single parameter sets for *Acacia* hybrids, *Eucalyptus* hybrids and *Pinus taeda* have been used by the 3-PG model (Physiological Principles Predicting Growth) to simulate their responses across wide ranges of soils, climates and silvicultural treatments (Almeida et al., 2010; Gonzalez-Benecke et al., 2016; Hung et al., 2016). This also enables the use of data from monocultures to parameterize and calibrate models to be used for mixtures when there is no empirical data available for the given mixture.

The 3-PG model (Landsberg and Waring, 1997) fits these three criteria. However, it has rarely been used for mixed-species forests (Forrester and Tang, 2016). Therefore, the first objective of this study was to (1) examine whether the recently developed mixed species version, 3-PG$_{mix}$, could predict the growth and yield of *Pinus sylvestris* and *Fagus sylvatica* forests distributed across 26 sites in Europe (Fig. 1), while using single parameter sets for each species. The second objective was to (2) test whether 3-PG$_{mix}$ could predict the mixing effects on the growth and yield of these *Pinus sylvestris* and *Fagus sylvatica* mixtures.
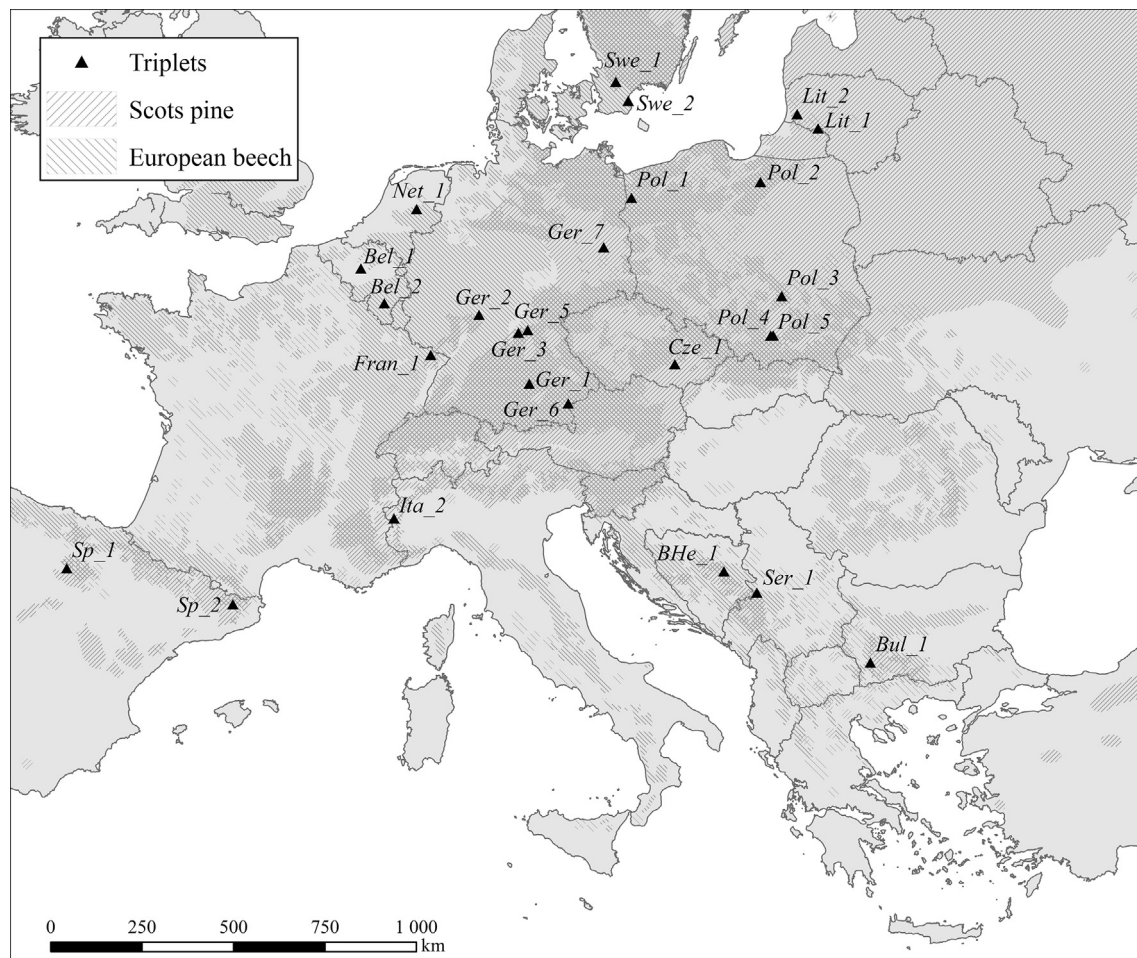

Fig. 1. The locations of the 26 sites, each with a triplet of plots of *Pinus sylvestris* and *Fagus sylvatica* in relation to their current distributions according to EUFORGEN (http://www.euforgen.org/distribution-maps/).

Previous studies that used the same plots found large variability in mixing effects, which were weakly correlated with site or climatic variables (Pretzsch et al., 2015a; del Río et al., 2017), although mixing effects for *P. sylvestris* were caused, at least partly, by light-related interactions (Forrester et al., in press). The unclear causality possibly resulted because multiple factors can cause the mixing effects and these cannot be teased apart using empirical data without a higher number of plots or detailed physiological measurements. Therefore, the third objective was (3) to use 3-PG$_{mix}$ to investigate which processes might be causing the mixing effects at the different sites and to examine whether 3-PG$_{mix}$ predicts how mixing effects change along gradients in climate, soil fertility, age and thinning intensity that are consistent with empirical studies about these species. Thinning intensity was considered because this is a main silvicultural treatment that could be used to modulate mixing effects (Bauhus et al., 2017b), and many studies have found that mixing effects can change with stand density (Garber and Maguire, 2004; del Río and Sterba, 2009; Condés et al., 2013; Forrester et al., 2013).

2. Methods

2.1. Site description

Model predictions were compared with data collected from 26 sites. At each site, there were three plots, including a mixture and monocultures of *P. sylvestris* and *F. sylvatica*. The sites were distributed along a productivity and rainfall gradient through Europe, through much of the overlapping area of the distributions of *P. sylvestris* and *F. sylvatica*. The southernmost sites are located in Spain and Bulgaria and the northernmost sites are in Sweden (Fig. 1). The plots were generally rectangular and ranged in size from 0.037 to 0.462 ha. Plot selection criteria were that they were as close as possible to even-aged, that they had not been thinned for at least ten years and that the trees were mostly mixed on a tree-by-tree basis. The stands were all semi-natural forests, as opposed to plantations. In addition, for a given site, all three plots had to be on a similar soil substrate, aspect and slope. The data and a more detailed description of the data are provided in Heym et al. (2017) and Heym et al. (in press).

At these locations the mean annual precipitation ranges from 520 to 1175 mm, the mean temperature from 6.0 to 10.5 °C and the elevation from 20 to 1339 m a.s.l. A site productivity index (*SI*) was calculated for each species as the height of the 100 largest-diameter trees of that species per hectare in monospecific stands at age 50 years (Pretzsch et al., 2015a). The *SI* ranged from 11.7 to 27.6 m for *F. sylvatica* and from 9.5 to 26.9 m for *P. sylvestris*. More detail about the climatic and edaphic conditions of each site is provided in Table A2 of Appendix A.

A wide range of stand structures was covered by the 78 plots at the 26 sites. In the mixtures, the percent of basal area that was *P. sylvestris* ranged from 28% to 73%. The basal area ranged from 13.3 to 78.0 m² ha⁻¹, the number of trees per hectare from 82 to 2649 and the stand age from 40 to 150 years.

2.2. Data collection

The diameters at 1.3 m of all trees were measured in each plot. The heights, height to the crown base and crown diameters were also measured for all trees or for a sample of trees (at least 10 randomly selected trees per species per plot). These measurements were conducted between autumn 2013 and spring 2014. Tree dimensions and annual growth for each year from 2002 to 2014 were calculated using increment cores that were collected from at least 20 trees per species per plot covering the diameter range for the given species and plot. The diameter increments of all non-cored trees were calculated by fitting diameter increment functions for each plot and species, where diameter increment was a function of diameter at 1.3 m and both were log-transformed. More detail is provided in Pretzsch et al. (2015a). The

crown diameters, heights and live-crown lengths of the trees that were not measured, or for years prior to 2014, were predicted using site- and species-specific allometric equations that were developed in another study using the same plots (Forrester et al., in press). Plot biomass (stems, foliage and roots) was estimated using generalized biomass relationships for *F. sylvatica* and *P. sylvestris* that incorporate the effects of stand basal area, trees per ha and age (Forrester et al., 2017b).

2.3. Description of 3-PG$_{mix}$

The 3-PG model was developed by Landsberg and Waring (1997) and since then it has been validated for many species and regions around the world (Landsberg and Sands, 2010). The original version of 3-PG was developed for monocultures but recent modifications have extended its use to mixed-species forests (3-PG$_{mix}$; Forrester and Tang, 2016), which are freely available as an Excel file at http://3pg.forestry.ubc.ca/. The input parameters and their units are listed in Table A1 of Appendix A and the types of species interactions that can be simulated are listed in Table 1. The 3-PG$_{mix}$ model has a monthly time step and consists of five sub-models in a causal chain starting with light absorption and assimilation and culminating with the conversion of biomass into output variables commonly used by foresters (Landsberg and Waring, 1997; Sands and Landsberg, 2002). The first sub-model predicts light absorption using the model described in Forrester et al. (2014) and then predicts gross primary production (*GPP*) using the maximum potential light-use efficiency (α_{Cx}). The α_{Cx} is reduced in response to limitations imposed by temperature, frost, vapour pressure deficit (*VPD*), soil moisture, soil fertility, atmospheric CO_2 and stand age (Landsberg and Waring, 1997; Sands and Landsberg, 2002; Almeida et al., 2004). Net primary production (*NPP*) is calculated assuming *NPP/GPP* = 0.47 (Waring et al., 1998).

The *NPP* is distributed to foliage, stems and roots by the second sub-model. Soil fertility, *VPD* and soil moisture influence partitioning to roots while partitioning between stems and foliage is influenced by tree size, with larger trees partitioning a lower proportion of *NPP* to foliage (Landsberg and Waring, 1997; Sands and Landsberg, 2002). The third sub-model calculates density-dependent mortality using the $-3/2$ self-thinning law (Yoda et al., 1963) to adjust the number of trees per ha (Landsberg and Waring, 1997; Sands and Landsberg, 2002). Density-independent mortality can also be predicted (Sands, 2004; Gonzalez-Benecke et al., 2014). The water balance is predicted by the fourth sub-model. Canopy conductance g_c is calculated using a species-specific maximum g_c, leaf area index (*LAI*) and any limitations caused by *VPD*, soil moisture, atmospheric CO_2 and stand age. The former two can vary along vertical gradients within the canopy depending on the vertical distribution of foliage. Transpiration and soil evaporation are calculated using the Penman–Monteith equation and these are added to canopy interception to predict evapotranspiration. Soil water is calculated as the difference between evapotranspiration and rainfall, with any water in excess of the maximum soil water holding capacity being drained off (Sands and Landsberg, 2002). If evapotranspiration is greater than the available soil water, the *NPP* is reduced. The fifth sub-model converts biomass into output variables such as mean tree diameter, height, basal area, wood volume, etc.

The calculation of species mixing proportions is required for several relationships in 3-PG$_{mix}$ and these proportions must be calculated using appropriate variables (Forrester and Tang, 2016). For example, the total stand *LAI* used to calculate canopy interception and canopy conductance is adjusted using mixing proportions based on species contributions to stand *LAI*. Whereas the number of trees per ha (*N*) used for self-thinning calculations is adjusted based on the mixing proportions in terms of stem mass because the equation describing the self-thinning law is based on stem mass.

To simulate the dynamics of deciduous species, two parameters are required that define the month when leaves are produced (*leaf$_P$*) and the month when they are lost (*leaf$_L$*) (Forrester and Tang, 2016). Leaves
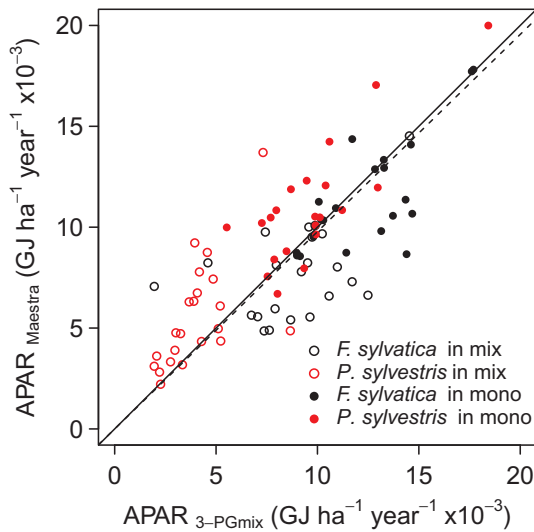
Fig. 2. Comparison of predicted absorption of photosynthetically active radiation by Maestra (APAR$_{Maestra}$) and 3-PG$_{mix}$ (APAR$_{3-PGmix}$) for the year 2014. The solid line is a 1:1 line and the dashed line is fitted to the data that passes through the origin.

are lost at the beginning of month *leaf*$_L$ and the foliage biomass (*WF,* Mg ha^{-1}) that was lost at the start of *leaf*$_L$ will be produced again at the end of month *leaf*$_P$. At the start of the growing season, all *NPP* is partitioned to *WF* (none to stems *WS* or roots *WR;* both Mg ha^{-1}) until an NPP equal to the *WF* has been produced, and after that, NPP will be partitioned to *WS, WF* and *WR*. For a full description of 3-PG$_{mix}$ please see Forrester and Tang, 2016.

2.4. Parameterisation

Most parameters were estimated using data collected in the plots and from published studies, as indicated in Table A1 and described below. A small number of parameters were fitted, including those that define biomass partitioning between foliage and stems (*p*$_2$, *p*$_{20}$), the minimum and maximum partitioning to roots (η_{Rx} and η_{Rn}) and the litterfall rates (γ_{Fx} and γ_R). This model calibration was firstly done using monospecific plots, with 3-PG$_{mix}$ initialised with the stand structure that existed in each plot in 2002 in terms of species-specific age, foliage mass, stem mass, root mass and trees per ha. The 3-PG$_{mix}$ model was then run for 11 years and the predictions for 2013 were compared with the measured values. One parameter was changed at a time until predicted diameter, height, basal area and biomass variables from monocultures were as close as possible to those estimated in the plots.

2.5. Meteorological data

The 3-PG$_{mix}$ model requires monthly weather data. This was obtained from the ERA-Interim reanalysis daily data, which was used to provide monthly weather data (from 2002 to 2014) with a spatial resolution of 0.125° latitude × 0.125° longitude, ≈10 km × 10 km, depending on the latitude (Dee et al., 2011). This is the latest global atmospheric reanalysis dataset produced by the European Centre for Medium-Range Weather Forecasts. The climatic variables included monthly mean daily minimum, maximum and mean temperature, precipitation and solar radiation. The use of ERA-Interim data instead of site-specific data could add error to the 3-PG$_{mix}$ predictions. No weather stations were located at the sites but solar radiation (the most difficult weather variable to obtain) from weather stations that were close to three of the sites, was highly correlated (R^2 > 0.7) with the ERA-Interim data.

2.6. Allometric relationships

In contrast to the individual tree allometric relationships described in "*Data collection*", 3-PG$_{mix}$ predicts mean height ($\bar{h}$, m), mean live-crown length ($\bar{h}_L$, m) and mean maximum crown diameter ($\bar{K}$, m) to quantify the canopy structure in order to predict light absorption and the vertical gradients in climatic conditions within the canopy (Forrester and Tang, 2016). These are predicted in 3-PG$_{mix}$ as functions of mean stem diameter at 1.3 m ($\bar{B}$, cm), relative height (*rh*, height of the target species divided by the mean height of all species in the plot), age (*A*, years) and competition (Eqs. (3)–(5)) using data from the mixed and monospecific plots,

$$\ln(h) = \ln(a_H) + n_{HB} \times \ln(B) + n_{HC} \times \ln(C) \tag{3}$$

$$\ln(h_L) = \ln(a_{HL}) + n_{HLB} \times \ln(B) + n_{HLrh} \times \ln(rh) + n_{HLC} \times \ln(C) \tag{4}$$

$$\ln(K) = \ln(a_K) + n_{KB} \times \ln(B) + n_{Krh} \times \ln(rh) + n_{KC} \times \ln(C) \tag{5}$$

where all a_x or n_x parameters are constants. The competition index (*C*) is calculated as the sum of the species-specific products of basal area and wood density using Eq. (6) (Forrester and Tang, 2016), which is assumed to reflect the current competition in relation to leaf area or sapwood area and hence light, transpiration and metabolic activity (Forrester et al., 2017a).

$$C = \sum_{i=1}^{n} BA_i \times \rho_i \tag{6}$$

where *BA* is the basal area (m^2 ha^{-1}) and ρ is the wood density (g cm^{-3}) of species *i*. The *C* is then expressed per ha after dividing by plot area (m^2).

Eqs. (3)–(5) were fitted for each species as mixed models, with plot nested within site as the random structure, using the *nlme* package for fitting the mixed models (Harrison et al., 2009) with R 3.2.1 (R Core Team, 2016). To correct for the bias when back-transforming the response variables, a correction factor was calculated as the sum of the measured values divided by the sum of the (back-transformed) predicted values (Snowden, 1991). The back-transformed constants (a$_H$, a$_{HL}$ and a$_K$) need to be adjusted by multiplying by the correction factors.

The parameters that describe the relationship between individual tree stem mass *w$_s$* and diameter (*a$_S$* and *n$_S$*) were obtained from Forrester et al. (2017b), as were the parameters describing the relationship between age and specific leaf area. The mean wood density was estimated from values found in the literature (*P. sylvestris*; Landsberg et al., 2005; Xenakis et al., 2008) (*F. sylvatica*; Barbaroux, 2002; Cienciala et al., 2005; Gryc et al., 2008; Skovsgaard and Nord-Larsen, 2012). There was no relationship between wood density and age and therefore the wood density was assumed to be constant for each given species, as also assumed in studies where 3-PG was applied to *P. sylvestris* in northern Europe (Landsberg et al., 2005; Xenakis et al., 2008). In this study, the wood density is only used by 3-PG$_{mix}$ to calculate the competition index (Eq. (6)).

2.7. Quantum yield and biomass partitioning

The efficiency with which photosynthetically active radiation (*PAR*) is used to produce biomass (canopy quantum efficiency, α_{Cx}) was estimated by determining the maximum volume growth rates of these species, converting this to *NPP* using wood density and biomass expansion factors (Lehtonen et al., 2004; Vande Walle et al., 2005), adding litterfall estimates based on Lehtonen et al. (2004) (not for the deciduous *F. sylvatica*) and converting this to *GPP* assuming a ratio of *NPP/GPP* of 0.47 (Waring et al., 1998). This *GPP* was divided by the absorbed *PAR* (*APAR*) based on estimates in the same plots by Forrester et al. (in press), which also provided the light extinction coefficient parameters (*k$_H$*). The maximum volume growth rates were the
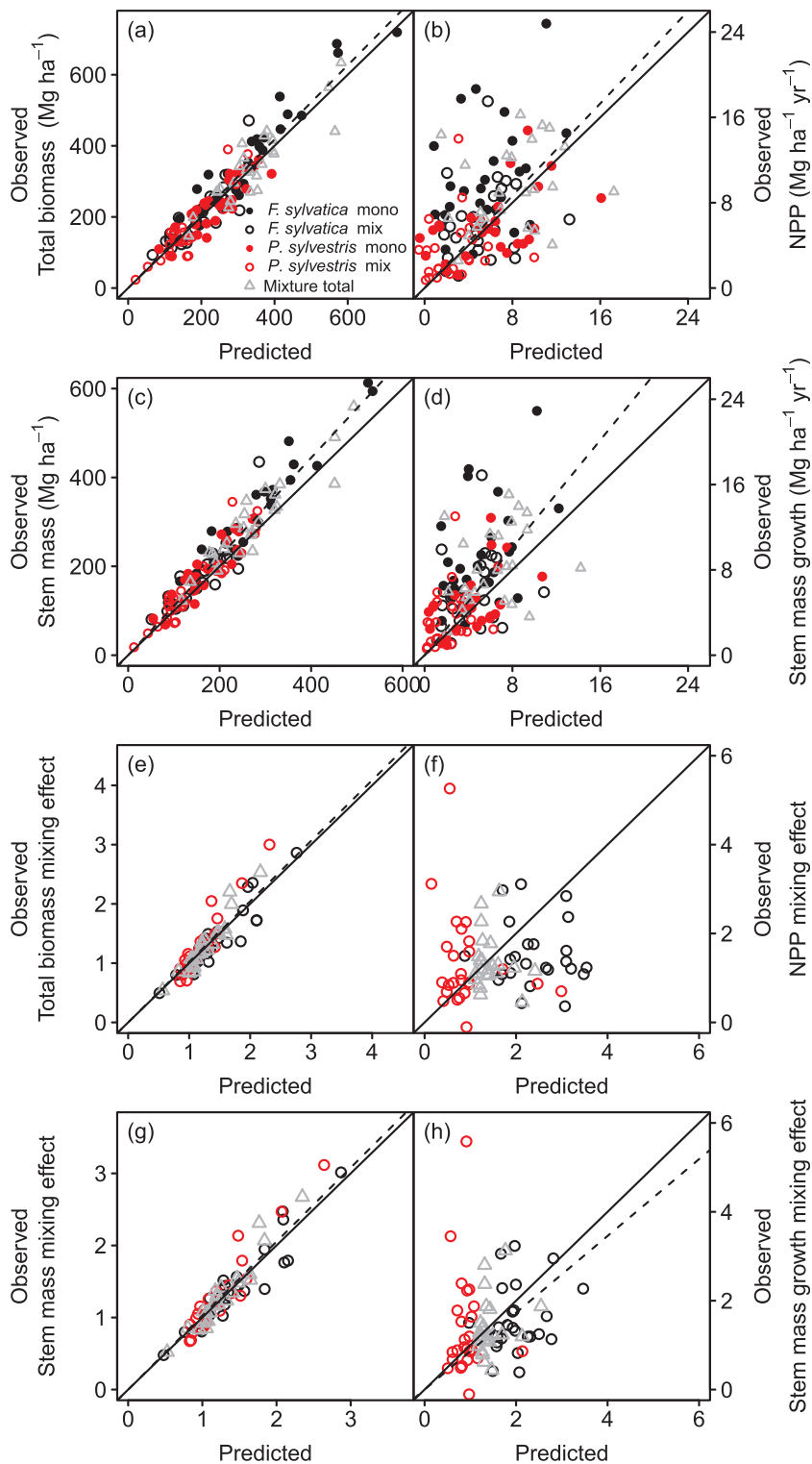
Fig. 3. Comparison of observed and predicted total biomass (TB, a), net primary productivity (NPP, b), stand stem mass (W$_S$, c), stem mass growth (d), the mixing effects, in terms of relative productivity (RP, Eqs. (1) and (2)) for total biomass (TB, e), net primary productivity (NPP, f), stand stem mass (W$_S$, g) and stem mass growth (h). Growth is for the year 2012 and stocks are for the end of 2012. The solid lines are 1:1 lines and the dashed lines are lines fitted to the data that pass through the origin. For each species-treatment combination n = 26.

maximum current annual increments in yield tables for southwestern Germany (Bösch, 2003), where these species are considered to grow under optimum conditions.

The *leaf*$_P$ and *leaf*$_L$ parameters, which describe when deciduous species (*F. sylvatica*) produce and lose their leaves were obtained from local foresters (Table A2 of Appendix A). The temperature limits on α (T$_{min}$, T$_{opt}$, T$_{max}$) were approximations based on San-Miguel-Ayanz et al. (2016) and Felbermeier and Mosandl (2014) while the default frost effects were used (k$_F$ = 1). Maximum stand age parameters of 350 years (*P. sylvestris*) and 300 years (*F. sylvatica*) were applied

(Faliński, 1986; Felbermeier and Mosandl, 2014). The default value for the effects of vapour pressure deficit on g$_c$ (k$_D$) was used for *P. sylvestris* (Landsberg et al., 2005; Xenakis et al., 2008). The k$_D$ for *F. sylvatica* was the mean of values calculated from Jonard et al. (2011) and Köcher et al. (2009).

2.8. Self-thinning and size distributions

Negligible self-thinning had occurred during the past decade in the plots used in this study. Therefore, the density-dependent mortality
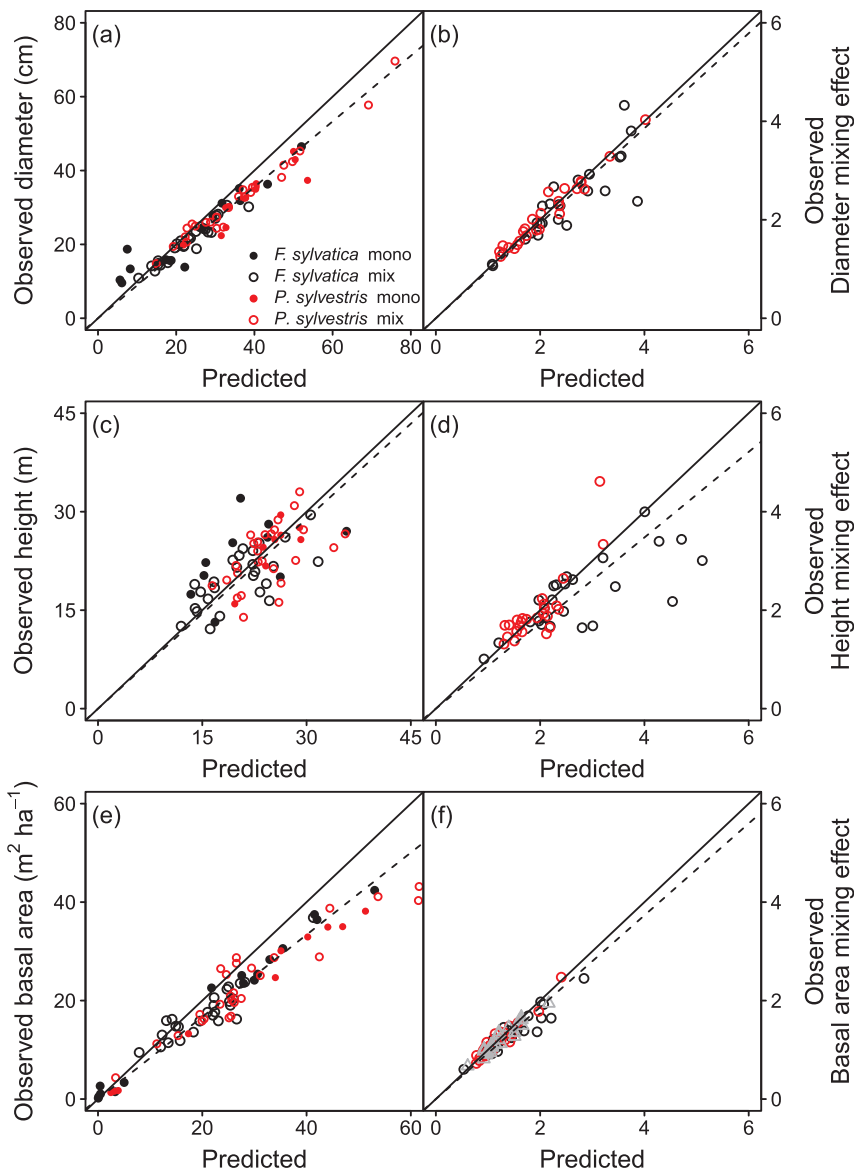
Fig. 4. Comparison of observed and predicted diameter at 1.3 m (a), the mixing effect in terms of relative productivity (RP) of diameter (b), height (c), RP of height (d), basal area (e) and RP of basal area (f). All data is for the end of 2012. The solid lines are 1:1 lines and the dashed lines are lines fitted to the data that pass through the origin. For each species-treatment combination n = 26.

parameter, w_{Sx1000}, was set high (400) for each species to prevent any mortality. If required, these parameters can be calculated from previous studies (Pretzsch, 2005; Condés et al., 2017). There was also no evidence or information about density-independent mortality, so these parameters were set at 0.

The 3-PG$_{mix}$ model uses diameter B (cm) and stem mass w_S (kg) Weibull distributions to correct the bias due to Jensen's Inequality that results from using allometric equations (Forrester and Tang, 2016); the mean of a function is not the same as the function of the mean (Duursma and Robinson, 2003). The location, scale and shape parameters of the Weibull distributions were predicted as functions of mean diameter, relative height (height of the target species divided by the mean height of all species in the plot), age and the competition index (Eq. (6)). In the mixtures, the number of trees in each class was adjusted by dividing by the mixing proportion of the given species, based on its contribution to stand basal area. The variables in these equations were log-transformed, which was not the case for the original 3-PG$_{mix}$ model (Forrester and Tang, 2016). The distributions and the Weibull equations are described in Appendix B.

2.9. Rainfall interception

The maximum proportion of rainfall intercepted by the canopy (I_{Rx}) of a given species monoculture was estimated from the mean of values found in the literature for these species (*F. sylvatica*: Nihlgård, 1970; Augusto et al., 2002; Staelens et al., 2006; Staelens et al., 2008; Barbier et al., 2009; Gerrits et al., 2010) (*P. sylvestris*: Rutter, 1963; Gash and Stewart, 1977; Alcock and Morton, 1981; Cape et al., 1991; Augusto et al., 2002; Barbier et al., 2009; Van Nevel, 2015). An *LAI* of 3 for maximum rainfall interception (L_{Ix}) was used based on the patterns shown in the rainfall interception studies cited above that included values of *LAI*.

2.10. Estimating soil fertility

Soil fertility for 3-PG$_{mix}$ is quantified using a fertility rating (FR). When available, site productivity indices and yield tables can provide a good overall estimate of the growing conditions for monocultures. SI

Table 2

Statistical information that describes the relationships between the predicted and observed variables for mixtures (plain font) or monocultures (bold font) as shown in Figs. 3, 4 and 3B. The monocultures were used to calibrate the model and the mixtures were used to validate the model. NPP = net primary productivity, W_S = stem mass, W_R = root mass. The statistical information includes the relative average error (e%), the relative mean absolute error (MAE%), the mean square error (MSE), the model efficiency (EF), the slope of the relationship forced through the origin, the *P*-value for the test of whether the slope of the relationship is significantly different from 1, and the R^2 values. Foliage growth and root growth are not considered due to the low reliability of calculating those variables using allometric equations.

Treatment	Species	Variable	e%	MAE%	MSE	EF	Slope	P-value	R^2
Mixture	*F. sylvatica*	Basal area	17.3	20.4	17.99	0.39	0.84	< 0.0001	0.98
Mixture	*P. sylvestris*	Basal area	22.8	25.4	62.4	0.29	0.78	< 0.0001	0.98
Mixture	Mixture total	Basal area	20.5	20.7	125.72	0.12	0.81	< 0.0001	0.99
Monoculture	***F. sylvatica***	**Basal area**	**11.5**	**14.9**	**39.17**	**0.54**	**0.87**	**< 0.0001**	**0.99**
Monoculture	***P. sylvestris***	**Basal area**	**17.1**	**21.5**	**85.53**	**0.09**	**0.84**	**< 0.0001**	**0.98**
Mixture	*F. sylvatica*	Diameter	10.9	11.4	9.59	0.67	0.89	< 0.0001	0.99
Mixture	*P. sylvestris*	Diameter	11.4	12.2	23.6	0.83	0.89	< 0.0001	1
Monoculture	***F. sylvatica***	**Diameter**	**3.6**	**16.9**	**21.01**	**0.76**	**0.91**	**0.0009**	**0.97**
Monoculture	***P. sylvestris***	**Diameter**	**13.4**	**14.9**	**26.16**	**0.66**	**0.87**	**< 0.0001**	**0.99**
Mixture	*F. sylvatica*	Height	2.7	14.7	13.43	0.25	0.95	0.1598	0.97
Mixture	*P. sylvestris*	Height	5	15.7	20.51	0.03	0.94	0.0901	0.97
Monoculture	***F. sylvatica***	**Height**	**−7.2**	**22.2**	**31.74**	**−0.44**	**1.02**	**0.725**	**0.94**
Monoculture	***P. sylvestris***	**Height**	**2.7**	**13.4**	**15.29**	**0.5**	**0.98**	**0.4642**	**0.97**
Mixture	*F. sylvatica*	W_S	−12.7	16.4	1719.55	0.67	1.14	0.0017	0.97
Mixture	*P. sylvestris*	W_S	−8.9	15.1	968.68	0.84	1.11	0.0094	0.97
Mixture	Mixture total	W_S	−11.1	14.1	4513.11	0.74	1.13	0.0012	0.97
Monoculture	***F. sylvatica***	**W_S**	**−12.5**	**13.6**	**1962.85**	**0.94**	**1.12**	**< 0.0001**	**0.99**
Monoculture	***P. sylvestris***	**W_S**	**−7.3**	**13.2**	**802.2**	**0.9**	**1.07**	**0.0102**	**0.98**
Mixture	*F. sylvatica*	W_S growth	−28.6	50.2	14.79	−0.36	1.18	0.2776	0.68
Mixture	*P. sylvestris*	W_S growth	−35.8	60	8.56	−0.22	1.21	0.3436	0.55
Mixture	Mixture total	W_S growth	−31.2	45.8	36.81	−0.26	1.3	0.0796	0.71
Monoculture	***F. sylvatica***	**W_S growth**	**−43.4**	**53.1**	**24.49**	**0.23**	**1.57**	**0.0002**	**0.76**
Monoculture	***P. sylvestris***	**W_S growth**	**22.7**	**100.3**	**44.17**	**0.12**	**0.87**	**0.6387**	**0.25**
Mixture	*F. sylvatica*	Total biomass	−4.7	15.1	1796.76	0.71	1.05	0.2749	0.96
Mixture	*P. sylvestris*	Total biomass	−1.2	16.9	1430.82	0.82	1.03	0.5098	0.96
Mixture	Mixture total	Total biomass	−3.2	13	4819.96	0.77	1.04	0.2529	0.97
Monoculture	***F. sylvatica***	**Total biomass**	**−8.6**	**12.8**	**2155.51**	**0.95**	**1.09**	**< 0.0001**	**0.99**
Monoculture	***P. sylvestris***	**Total biomass**	**3.9**	**15**	**1150.63**	**0.9**	**1.04**	**0.1362**	**0.98**
Mixture	*F. sylvatica*	NPP	−18.5	49.1	16.56	−0.36	1.03	0.8551	0.68
Mixture	*P. sylvestris*	NPP	−27.7	65	12.38	−0.5	0.91	0.6374	0.47
Mixture	Mixture total	NPP	−22	43.2	41.9	−0.29	1.12	0.4352	0.7
Monoculture	***F. sylvatica***	**NPP**	**−42.6**	**55.9**	**30.74**	**0.17**	**1.49**	**0.002**	**0.72**
Monoculture	***P. sylvestris***	**NPP**	**49.7**	**104.9**	**60.03**	**0.09**	**0.71**	**0.1695**	**0.27**
Mixture	*F. sylvatica*	RP − Basal area	17.3	20.4	17.99	0.39	0.84	< 0.0001	0.98
Mixture	*P. sylvestris*	RP − Basal area	22.8	25.4	62.4	0.29	0.78	< 0.0001	0.98
Mixture	Mixture total	RP − Basal area	20.5	20.7	125.72	0.12	0.81	< 0.0001	0.99
Mixture	*F. sylvatica*	RP − diameter	5.4	11.2	0.17	0.71	0.94	0.058	0.98
Mixture	*P. sylvestris*	RP − diameter	−0.3	5.2	0.02	0.95	1	0.9049	1
Mixture	*F. sylvatica*	RP − height	19.2	23.1	0.69	−0.45	0.79	< 0.0001	0.94
Mixture	*P. sylvestris*	RP − height	−2.1	12.1	0.14	0.69	1.03	0.4353	0.97
Mixture	*F. sylvatica*	RP − W_R	27.8	31.5	0.19	−0.92	0.78	< 0.0001	0.96
Mixture	*P. sylvestris*	RP − W_R	−12.1	20.8	0.13	0.26	1.15	0.0251	0.93
Mixture	Mixture total	RP − W_R	3.8	13	0.04	0.52	0.97	0.3788	0.97
Mixture	*F. sylvatica*	RP − W_S growth	28.4	50.2	0.83	−0.54	0.75	0.0025	0.81
Mixture	*P. sylvestris*	RP − W_S growth	−34.5	57.3	1.68	−0.29	1.35	0.2047	0.51
Mixture	Mixture total	RP − W_S growth	10.3	43.6	0.64	−0.06	0.89	0.3024	0.73
Mixture	*F. sylvatica*	RP − W_S	1.8	10.9	0.04	0.87	0.99	0.6051	0.98
Mixture	*P. sylvestris*	RP − W_S	−4.1	13.2	0.05	0.85	1.07	0.0393	0.98
Mixture	Mixture total	RP − W_S	−2.4	8.6	0.03	0.88	1.04	0.1027	0.99
Mixture	*F. sylvatica*	RP − Total biomass	4.7	11.8	0.05	0.83	0.96	0.1527	0.98
Mixture	*P. sylvestris*	RP − Total biomass	−6.5	13.6	0.06	0.78	1.1	0.0085	0.98
Mixture	Mixture total	RP − Total biomass	−1.8	8.8	0.03	0.85	1.04	0.1768	0.99

indicate the combined effect of different climatic, edaphic and biotic conditions. Therefore, the SI can be described as a function of climate, soil water properties and soil nutrition as shown in Eq. (7).

$$SI = \beta_0 + \beta_1 ASW + \beta_2 Martonne + \varepsilon \qquad (7)$$

where Martonne is the aridity index of each site according to de Martonne (1926), i.e., annual precipitation in mm/(mean annual temperature in °C + 10), which varied from 28 to 61, and ASW is the potential available soil water (mm). The potential ASW was calculated from the soil depth, the water holding capacity of the given soil's texture (mm/m) and the proportion of soil volume that is stones. The FR and SI are assumed to represent long-term average conditions and

therefore the de Martonne index was calculated from the long-term averages. It was assumed that any variability in SI that was not explained by soil water characteristics (ASW) or climate (de Martonne aridity index) was due to soil fertility and therefore ε provides an index of soil fertility (FR). Therefore, the FR is the observed SI plus the residual, and the residual is the observed SI minus the predicted SI from Eq. (7). This was then normalised so that the FR values lie between 0 and 1. Since species interactions can modify soil fertility (Richards et al., 2010), the FR values were only calculated using data from the monocultures, and the resulting FR values were also used in the mixtures. Besides the FR, default parameters for the fertility effects on productivity were used, except for f_{N0}, which describes the lowest relative fertility, namely 0.2 for *P. sylvestris* and 0.5 for *F. sylvatica*.
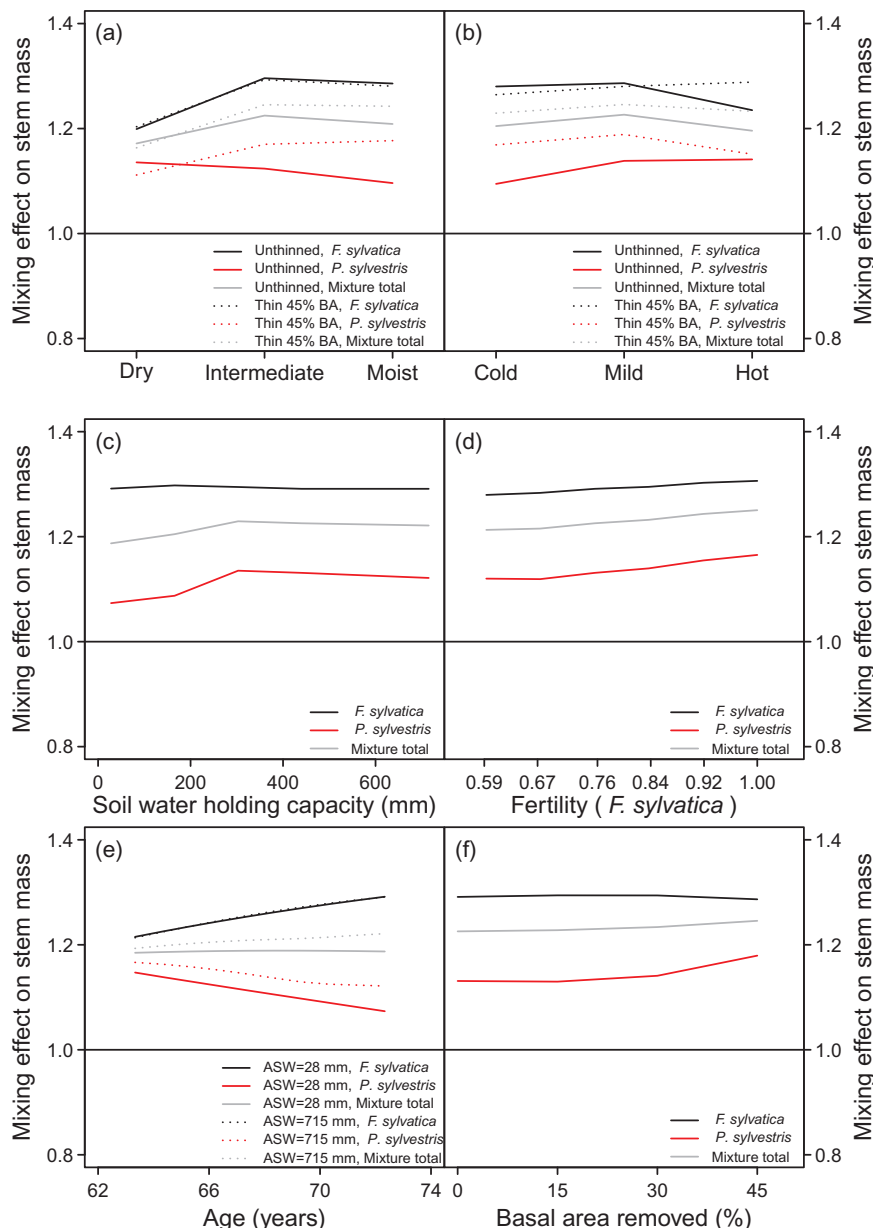
Fig. 5. The simulated mixing effect, in terms of the relative productivity (RP, Eqs. (1) and (2)) calculated using stem mass (W_S) along gradients in terms of precipitation (a), temperature (b), soil water holding capacity (c), soil fertility (d), age (e) and thinning intensity (f). The levels of each gradient are described in the text. If RP is > 1 then the W_S was greater in mixture than monoculture, whereas if RP is < 1 the W_S was lower in the mixture than in monoculture. Except for (e), all patterns are only shown for the final year of the simulation (2013). Soil fertility (FR) for both species were linearly correlated so only *F. sylvatica* is shown on the x-axis in (d). ASW indicates the available soil water holding capacity for the simulated site.

2.11. Evaluation of model performance

To test the light absorption predictions from 3-PG$_{mix}$, its predictions were compared with those from Maestra (Medlyn, 2004), which is a much more detailed tree-level model. Maestra predicts the light absorption of all individual trees within a stand. It uses individual tree positions (x- and y-coordinates), the site slope and individual tree dimensions (crown diameter, length, height and leaf area) to determine the canopy structure and thereby accounts for shading by neighbouring trees. Maestra accounts for intra- or inter-specific differences in crown architecture in terms of crown dimensions, the vertical distribution of leaf-area density, the leaf angle distribution and the optical properties of leaves. The predictions from Maestra were obtained from another study in the same plots that examined how light absorption was influenced by tree allometry, tree size and stand structure (Forrester et al., in press). The Maestra light absorption predictions compared well with light absorption predicted for the same plots using hemispherical photos, with $R^2 = 0.67$ and a slope (forced through origin) for the relationship between observed vs. predicted values of 0.92 (see Fig. S3 in Forrester et al., in press). Maestra light absorption predictions have also

been validated in other mixed-species stands (Charbonnier et al., 2013; le Maire et al., 2013). The parameterisation of Maestra for these plots is described in detail in Forrester et al. (in press).

The 3-PG$_{mix}$ output variables basal area, stem mass, leaf mass, root mass, diameter, height, APAR and mixing effects (Eqs. (1) and (2)) on these variables were compared with the estimates from the plot measurements (mass variables were calculated using allometric biomass equations, as described above). The model was initialised with the stand structure that existed in each plot in 2002 in terms of species-specific age, foliage mass, stem mass, root mass and trees per ha. It was then run for 11 years and the predictions for 2013 were compared with the measured values. Given that the monospecific plots were used to parameterise and calibrate the model, a validation was performed using the mixed-species plots, before finally combining the data from the mixtures and monocultures to obtain the final parameter set. The criteria used to make comparisons included the relative average error (average bias, $e\%$, Eq. (8)), the relative mean absolute error (MAE%, Eq. (9)), the mean square error (MSE, Eq. (10)) (Janssen and Heuberger, 1995; Vanclay and Skovsgaard, 1997) and the model efficiency (EF, Eq. (11)) (Loague and Green, 1991), which can be less than
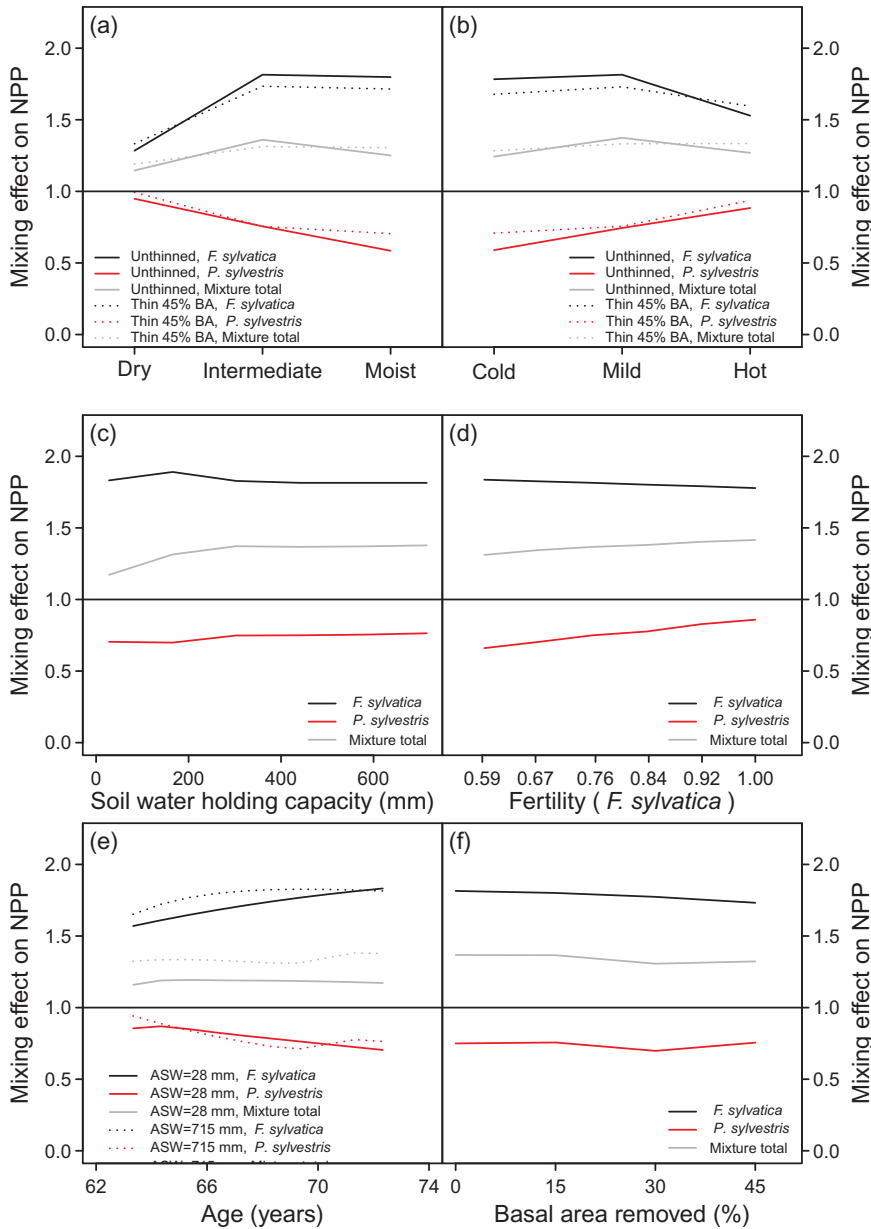
Fig. 6. The simulated mixing effect, in terms of the relative productivity (RP, Eqs. (1) and (2)) calculated using NPP along gradients in terms of precipitation (a), temperature (b), potential available soil water (c), soil fertility (d), age (e) and thinning intensity (f). The levels of each gradient are described in the text. If RP is > 1 then the NPP was greater in mixture than mono-culture, whereas if RP is < 1 the NPP was lower in the mixture than in monoculture. Except for (e), all patterns are only shown for the final year of the simulation (2013). Soil fertility (FR) for both species were linearly correlated so only *F. sylvatica* is shown on the x-axis in (d). ASW indicates the available soil water holding capacity for the simulated site.

zero (indicating a poorer model prediction than simply using the mean) up to a maximum of 1, where there is a perfect correlation between predictions and observations.

$$e\% = 100\frac{\widetilde{P}-\widetilde{O}}{\widetilde{O}} \tag{8}$$

$$MAE\% = 100\frac{((\sum_{i=1}^{n}|P_i-O_i|)/n)}{\widetilde{O}} \tag{9}$$

$$MSE = \frac{\sum_{i=1}^{n}(P_i-O_i)^2}{n} \tag{10}$$

$$EF = \frac{\sum_{i=1}^{n}(O_i-\widetilde{O})^2 - \sum_{i=1}^{n}(P_i-O_i)^2}{\sum_{i=1}^{n}(O_i-\widetilde{O})^2} \tag{11}$$

where O_i are the observed values, P_i are the predicted values from 3-PG$_{mix}$, and $\widetilde{O}$ and $\widetilde{P}$ are the means. All statistical analyses were performed using R 3.2.1 (R Core Team, 2016).

2.12. Simulation of the spatial and temporal dynamics of species interactions

3-PG$_{mix}$ was then used to simulate the effects of climate, soil fertility, soil water holding capacity, stand age and thinning intensity on mixing effects. To initialise the stands, we used the mean ages, mean species-specific stem mass, root mass, foliage mass and trees per ha in 2002. That is, we used a single "mean" stand structure to initialise all simulations. The final year of the simulations was 2013. A factorial design was used, including 3 species compositions (2 monocultures + 1 mixture) × 6 climates (3 levels of temperature and 3 levels of pre-cipitation) × 6 fertility levels × 6 levels of soil water holding capa-city × 4 levels of thinning intensity = 2592 simulations that each went for a duration of 13 years, from age 61 to 73 years (2002 to 2013).

The climates for the temperature gradient were obtained by se-lecting the climate data from two or three sites with the lowest, medium and highest mean monthly maximum temperatures. Then the mean monthly climate values (from 2002 to 2014) for each given category (low, medium or high) were used to obtain three climatic scenarios with low, medium and high temperatures. A similar procedure was used

to obtain three climatic scenarios with low, medium and high annual precipitation. This precipitation gradient also represented a gradient in the terms of the de Martonne (1926) aridity index. Six levels of species-specific soil fertility were used, ranging from the lowest to the highest values calculated for all sites. The fertility was increased for both species simultaneously, because there was a positive correlation between the site productivity indices of each species (P = 0.017, R^2 = 0.25) (Forrester et al., in press). The 6 levels of maximum available soil water (mm) ranged from 28 to 715 mm, which was the range found across the sites in this study. Four thinning intensities were applied at the start of the simulations in 2002 such that 0%, 15%, 30% and 45% of the biomass (of both species) was removed.

3. Results

3.1. Validation

The *APAR* values predicted by 3-PG$_{mix}$ were well correlated (R^2 = 0.96) with predictions from the detailed tree-level model Maestra (Fig. 2). The slope of the regression line fitted to these data and forced through the origin (dashed line in Fig. 2) was 0.978, indicating an average overestimate by 3-PG$_{mix}$ of < 3% compared with Maestra. This level of accuracy is relatively high given that the plots covered a wide range of stand structures and leaf area index, and also given that 3-PG$_{mix}$ only uses species-specific means as inputs rather than spatially explicit individual tree information.

The 3-PG$_{mix}$ model produced accurate predictions of total biomass, stem mass and anything derived from them such as mean diameter and basal area, which were all highly correlated with the observed values (R^2 > 0.95, Figs. 3 and 4). For these variables, the predictions for both species were marginally more precise and less biased in the monocultures, which were used for model calibration, than in the mixtures. This was indicated by the mean e% (mono = 2.6, mix = 3.7), MAE% (mono = 15.4, mix = 16.4), MSE (mono = 789, mix = 1 408) and EF (mono = 0.72, mix = 0.62) (Table 2). The predictions of NPP and stem mass growth were more variable, for example e% was − 42.6 to 49.7 in monocultures but −18.5 to −35.8 in mixtures and the mean of MAE% was 79 in monocultures and 56 in mixtures. The predictions for growth rates or for variables that had much smaller magnitudes (i.e. foliage and roots), were much less precise (Figs. 3 and B3).

The predicted mixing effects (RP) on growth and yield followed similar patterns for all variables (Table 2). The mixing effects for total biomass, stem mass, basal area and diameter were generally precise (mean MAE% = 13.6) and with a low bias (mean e% = 5.2). In contrast, the predictions of mixing effects for foliage and root mass were not accurate (Fig. B3).

3.2. Simulations

Thinning increased the mixing effects for *P. sylvestris* and the total mixture stem mass (Fig. 5f) but reduced mixing effects on *F. sylvatica* NPP (Fig. 6f). Thinning also modified the effect of climate on mixing effects by reducing the differences between species as the thinning intensity increased (Figs. 5a, b and 6a, b). For stem mass, this response was more pronounced for *P. sylvestris* than *F. sylvatica*. Increasing soil fertility resulted in higher mixing effects on stem mass for *P. sylvestris* and the total mixture (Fig. 5d) but reduced the mixing effect on *NPP* for *F. sylvatica* (Fig. 6d). As the stands aged, the mixing effects were predicted to increase for *F. sylvatica* and decline for *P. sylvestris*, with the total mixture showing negligible changes (Figs. 5e and 6e). Drier or hotter climates reduced the mixing effect for *F. sylvatica* but increased the mixing effects for *P. sylvestris* (Figs. 5a, b and 6a, b).

4. Discussion

The 3-PG$_{mix}$ model was able to predict the growth and yield of

mixed-species plots after being calibrated using monocultures. It was also able to predict the mixing effects that were consistent with other studies about the same species.

4.1. Validation and applicability to the F. sylvatica and P. sylvestris forests of Europe

The plot network used in this study included a wide range of stand structures and tree allometry, resulting in a correspondingly large range of light regimes (Forrester et al., in press). Even with this complexity, the simple light sub-model of 3-PG$_{mix}$ provided adequate predictions of light absorption. This level of accuracy is acceptable given (i) the variability in stand structures and allometry, (ii) that the comparisons were made against predictions from another model (Maestra) instead of direct measurements of light absorption and (iii) that the light sub-model is a stand-level model that simplifies the canopy into cohorts and ignores any spatial clumping of species or trees. Adequate validation of light calculations are critical for the many forest growth models, including 3-PG$_{mix}$, that base their *NPP* calculations on light-use efficiency (McMurtrie et al., 1994; Landsberg and Waring, 1997; Mäkelä et al., 2008), and therefore depend on reliable predictions of light absorption for their growth and yield predictions.

3-PG$_{mix}$ accurately predicted biomass yield, basal area and mean tree dimensions at the end of the 11-year simulation period. This is partly evidence that the model was performing well, but also resulted because actual stand structures (as of 2002, stand ages of 30–140 years) were used to initialise the simulations, which improves the accuracy of predictions compared to starting with seedlings (Sands and Landsberg, 2002). A much lower precision was obtained for growth or small biomass components, such as roots and foliage, as has also been observed elsewhere (Paul et al., 2007) and is expected due to the small sizes of these biomass components combined with their much greater relative variability (Forrester et al., 2017b).

Regardless of the size of the biomass components, there are several additional sources of error that should be considered. Firstly, the "observed" biomass data were predicted using allometric equations. These equations were developed using an independent European-wide data set and accounted for age, tree diameter and several stand structural characteristics that probably account for much of the mixing effects on allometry (Forrester et al., 2017a; Forrester et al., 2017b). Nevertheless, they are unlikely to be as accurate as site-specific destructively sampled biomass measurements. For example, in even-aged stands, such as those in this study, growth and foliage mass tend to decline after peaking when the stands are young (Ryan et al., 1997). *F. sylvatica* leaf area index was declining along an age series from 80 to 160 years in Germany (Leuschner et al., 2006) and yield tables of southwestern Germany indicate that volume increments decline after peaking at ages 35–45 years for *P. sylvestris* and 65–85 years for *F. sylvatica*, with peaks occurring earlier on more productive sites (Bösch, 2003). Given the current ages of these stands (40–150 years) the growth rates and foliage mass at many of the sites are likely to be showing long-term trends of decline. Even with age as an independent variable, these tree-level allometric equations may not be precise enough to capture this stand-level variability. 3-PG$_{mix}$ is probably more sensitive to differences in site, age and stand structural conditions than the allometric equations and therefore the error and bias of the 3-PG$_{mix}$ biomass predictions was probably overestimated.

A second source of error is the potential for genetic variability of the 3-PG$_{mix}$ parameters. The physiology, morphology and phenology of *F. sylvatica* and *P. sylvestris* probably changed along the transect in relation to the different climatic and edaphic conditions (Rehfeldt et al., 2002; Robson et al., 2012). That is, the *P. sylvestris* trees in Sweden probably differ to the *P. sylvestris* in Spain, but when calculating the parameter values, data from a wide range in the distributions were combined into a mean value for each parameter; there were not enough data to develop region-specific parameter sets. Process-based models are rarely

applied across such large natural distributions of a single species and therefore an effect of genetic variability cannot be compared with other studies.

Most forest growth models, regardless of whether they are empirical or process-based, face the problem of systematic genetic variability (in physiology/morphology/phenology) when applied across an area large enough to include multiple provenances of the given species. This genetic effect could be incorporated into models if the genetic influence on parameters varies systematically with climatic or edaphic conditions, otherwise different parameter sets will be required for each provenance. For example, clone-specific parameter sets are used when applying 3-PG to *Eucalyptus* plantations in south America (e.g., Almeida et al., 2004). Models applied to large areas that ignore systematic differences in physiological, morphological and phenological characteristics of a species may not be reliable for predicting many aspects of forest functioning, including species interactions and potential changes in species distributions. Similarly, parameter sets developed for a given species in one part of its natural distribution may not be reliable for the same species in another part of its natural distribution. The general European-wide parameters used in this study should be further refined when applied to specific regions. This refinement should target the parameters that are most likely to change and that 3-PG$_{mix}$ is most sensitive too, such as p_{20}, k_H, α_{Cx}, σ_1 (Forrester and Tang, 2016).

This does not mean that a single parameter set cannot be applied to large areas with wide ranges in climatic and edaphic conditions. For example, 3-PG is well known to provide very precise and less biased predictions using a single parameter set, when the genetic variability of the simulated species is relatively low, such as in plantations, even when the growing conditions span a wide range of climates, soil types and silvicultural treatments (Almeida et al., 2010; Gonzalez-Benecke et al., 2016; Hung et al., 2016). 3-PG has also already been shown to provide accurate predictions for *P. sylvestris* in northern Europe using parameters similar to those used in this study (Landsberg et al., 2005; Xenakis et al., 2008), and other stand-level forest growth models have also performed well using single parameter sets (Härkönen et al., 2010).

4.2. Comparison of simulations with published empirical observations

3-PG$_{mix}$ was designed specifically to include many of the species interactions that can influence the growth and functioning of mixed-species forests (Table 1). Even though it does not include all possible species interactions and all interactions are simulated at the stand level (not at the tree level), the predicted mixing effects compared well with the observed mixing effects at the 26 sites used for this study which covered a wide range in stand structures and climates. This suggests that the most influential processes driving the dynamics of these forests are included in 3-PG$_{mix}$ (Table 1). The predictions also compared well with other studies about these species. For example, as thinning intensity increased, the mixing effects were predicted to decline for *F. sylvatica* but increase for *P. sylvestris*. This pattern was also found in response to differences in stand density using a large dataset from Spain (Condés et al., 2013).

As soil fertility increased, the mixing effect was predicted to increase for *P. sylvestris*. Increasing mixing effects with increasing soil fertility are likely to result when species interactions improve light absorption or light-use efficiency (Forrester, 2014). Consistent with this prediction, another study that used the same plots found that the mixing effects for *P. sylvestris* growth were correlated with mixing effects on light absorption (Forrester et al., in press).

As the stands aged, the mixing effects were predicted to increase for *F. sylvatica* and decline for *P. sylvestris*. At the start of the simulation, age 62 years, the mean height of *P. sylvestris* was 21.5 m and *F. sylvatica*

was 15.6 m, but by the end of the simulation at age 73 years, the height difference was much smaller (22.7 and 20.7 m, respectively). Therefore, the vertical overlap between *F. sylvatica* and *P. sylvestris* crowns increased, which probably reduced the light complementarity effect experienced by *P. sylvestris*. This highlights the potential need for thinning *F. sylvatica* from the larger size classes to maintain the upper canopy position of *P. sylvestris* (Spathelf and Ammer, 2015). It is also important to note that the initial conditions used as inputs for 3-PG$_{mix}$ (e.g. species specific values of trees per hectare, biomass per ha, age) will influence the simulation. The mean conditions of all sites were used in this study in order to examine general patterns. However, if the actual dynamics for specific sites are of interest, then site-specific inputs are required. Similarly, the simulation in this study ran for 11 years, but a more reliable test could include a greater proportion of the rotation.

The effects of climate were also consistent with those reported in the literature. 3-PG$_{mix}$ predicted that mixing effects for *F. sylvatica* would be lowest at dry or hot sites, while those for *P. sylvestris* would be highest on those sites. This is consistent with a Spanish study on the same species (Condés and Río, 2015).

4.3. Conclusions

To our knowledge, this is the first time a forest growth model has been validated for its ability to predict mixing effects using empirical measurements of the mixing effects. This is despite the fact that most forests are mixed and that forest growth models are often applied to mixed-species forests. 3-PG$_{mix}$ predicted standing biomass well and predicted changes in mixing effects in response to soils, stand density, climate and age that matched measured data and case studies from the literature. Growth predictions were less precise than yield predictions, probably partly because the "observed" data were predicted using biomass equations (as opposed to more direct measurements) and because the parameter set was general for Europe and not site-specific.

Previous studies using the same plots found few clear spatial changes in mixing along the transect (Pretzsch et al., 2015a; del Río et al., 2017), except that the mixing effect on *P. sylvestris* growth was caused by light-related interactions (Forrester et al., in press). The difficulty in identifying significant patterns in previous studies was probably because multiple factors and processes influenced the mixing effects, and even with more than 30 sites (90 plots) distributed across Europe, it was not possible to disentangle these factors to show which processes were driving the mixing effects. 3-PG$_{mix}$ was used to tease apart the effect of climate, age and densities or thinning regimes on mixing effects and could therefore be used to identify which processes may have caused the mixing effects and which sites may be suitable or unsuitable for mixtures (Figs. 6 and B1).

Models such as 3-PG$_{mix}$ can be used to get an impression of the main processes and species interactions that drive mixing effects in forests and can facilitate the development of hypotheses, experimental designs and aid silvicultural decisions. Similarly, 3-PG$_{mix}$ could also be used to determine how experiments might need to be managed in the future, such as whether some species will need to be thinned to prevent them from dominating the other species or to maintain mixing effects at high levels.

Acknowledgements

Appendix A

See Tables A1 and A2.

Table A1

Description of parameters, their values and sources. Source refers to "Default" values for *Eucalyptus globulus* in 3-PG$_{PJS}$ 2.7, "Observed" values measured in this study or obtained from published observations, and "Fitted" values that were obtained, as described in the text. Sources for published observations are described in the methodology section.

Parameter	Symbol	Units	Source	*Pinus sylvestris*	*Fagus sylvatica*
Biomass partitioning and turnover					
Allometric relationships & partitioning					
Foliage:stem partitioning ratio @ B = 2 cm	p_2	–	Fitted	0.70	0.70
Foliage:stem partitioning ratio @ B = 20 cm	p_{20}	–	Fitted	0.21	0.06
Constant in the stem mass v. B relationship	a_S	–	Observed	0.126	0.183
Power in the stem mass v. B relationship	n_S	–	Observed	2.268	2.390
Maximum fraction of NPP to roots	η_{Rx}	–	Fitted	0.7	0.7
Minimum fraction of NPP to roots	η_{Rn}	–	Fitted	0.3	0.3
Litterfall & root turnover					
Maximum litterfall rate	γ_{Fx}	1/month	Fitted	0.015	0.02
Litterfall rate at t = 0	γ_{F0}	1/month	Default	0.001	0.001
Age at which litterfall rate has median value	$t_{\gamma F}$	months	Observed	60	60
Average monthly root turnover rate	γ_R	1/month	Fitted	0.004	0.015
If deciduous, the month when leaves produced	$leaf_P$	month	Observed	0	4
If deciduous, the month when leaves fall	$leaf_L$	month	Observed	0	11
NPP & conductance modifiers					
Temperature modifier (f_T)					
Minimum temperature for growth	T_{min}	°C	Observed	−5	−5
Optimum temperature for growth	T_{opt}	°C	Observed	15	20
Maximum temperature for growth	T_{max}	°C	Observed	35	25
Frost modifier (f_F)					
Days production lost per frost day	k_F	days	Default	1	1
Fertility effects					
Value of 'm' when FR = 0	m_0	–	Default	0	0
Value of 'f_N' when FR = 0	f_{N0}	–	Fitted	0.2	0.5
Power of (1-FR) in 'f_N'	n_{fN}	–	Default	1	1
Age modifier (f_{AGE})					
Maximum stand age used in age modifier	t_x	years	Observed	350	300
Power of relative age in function for f_{AGE}	n_{age}	–	Default	4	4
Relative age to give f_{AGE} = 0.5	r_{age}	–	Default	0.95	0.95
Canopy structure and processes					
Specific leaf area					
Specific leaf area at age 0	σ_0	m^2/kg	Observed	4.29	24.7
Specific leaf area for mature leaves	σ_1	m^2/kg	Observed	4.29	19.4
Age at which specific leaf area = (SLA0 + SLA1)/2	t_σ	years	Observed	1	35
Light interception					
Extinction coefficient for absorption of PAR by canopy	k or k_H	–	Observed	0.38	0.42
Age at canopy closure	t_c	years	Observed	10	10
Maximum proportion of rainfall evaporated from canopy	I_{Rx}	–	Observed	0.395	0.237
LAI for maximum rainfall interception	L_{Ix}	–	Default	3	3
LAI for 50% reduction of VPD in canopy	L_{50D}	–	Default	5	5
Production and respiration					
Canopy quantum efficiency	α_{Cx}	molC/molPAR	Observed	0.049	0.050
Ratio NPP/GPP	Y	–	Default	0.47	0.47
Conductance					
Minimum canopy conductance	g_{Cmin}	m/s	Default	0	0
Maximum canopy conductance	g_{Cmax}	m/s	Default	0.02	0.02
LAI for maximum canopy conductance	L_{gCmax}	–	Default	3.33	3.33
Defines stomatal response to VPD	k_D	1/mBar	Default/observed	0.05	0.057
Canopy boundary layer conductance	g_B	m/s	Default	0.2	0.2

Table A1 *(continued)*

Parameter	Symbol	Units	Source	*Pinus sylvestris*	*Fagus sylvatica*
Basic Density					
Minimum basic density – for young trees	ρ_0	t/m3	Observed	0.395	0.567
Maximum basic density – for older trees	ρ_1	t/m3	Observed	0.395	0.567
Age at which $\rho = (\rho_0 + \rho_1)/2$	t_ρ	years	Not applicable	1	1
Stem height					
Constant in the stem height relationship	a_H	–	Observed	4.589	1.008
Power of B in the stem height relationship	n_{HB}	–	Observed	0.474	0.450
Power of competition in the stem height relationship	n_{HC}	–	Observed	0	0
Crown shape					
Crown shape (1 = cone, 2 = ellipsoid, 3 = half-ellipsoid, 4 = rectangular)	–	–	Default	3	3
Crown diameter					
Constant in the crown diameter relationship	a_K	–	Observed	1.376	0.939
Power of B in the crown diameter relationship	n_{KB}	–	Observed	0.554	0.581
Power of height in the crown diameter relationship	n_{KH}	–	Observed	0	0
Power of competition in the crown diameter relationship	n_{KC}	–	Observed	−0.266	0
Power of relative height in the crown diameter relationship	n_{Krh}	–	Observed	0	0
Live-crown length					
Constant in the LCL relationship	a_{HL}	–	Observed	2.189	6.269
Power of B in the LCL relationship	n_{HLB}	–	Observed	0.563	0.189
Power of LAI in the LCL relationship	n_{HLL}	–	Observed	0	0
Power of competition in the LCL relationship	n_{HLC}		Observed	−0.262	0
Power of relative height in the LCL relationship	n_{HLrh}		Observed	0.678	0.655
Diameter distributions					
Constant for Weibull scale parameter of B dist.	sc_{B0}	–	Observed	0.278	0.194
Slope of DBH in relationship for Weibull scale parameter	sc_{BB}		Observed	1.152	1.225
Slope of relative height for Weibull scale parameter	sc_{Brh}		Observed	0	0
Slope of age in relationship for Weibull scale parameter	sc_{Bt}		Observed	0	0.128
Slope of competition for Weibull scale parameter	sc_{BC}		Observed	0.054	0
Constant in the relationship for Weibull shape parameter	sh_{B0}		Observed	1.228	0.788
Slope of DBH in relationship for Weibull shape parameter	sh_{BB}		Observed	0	0.316
Slope of relative height for Weibull shape parameter	sh_{Brh}		Observed	1.189	1.614
Slope of age in relationship for Weibull shape parameter	sh_{Bt}		Observed	0	0
Slope of competition for Weibull shape parameter	sh_{BC}		Observed	0.214	−0.117
Constant in the relationship for Weibull location parameter	loc_{B0}		Observed	0.987	1.636
Slope of DBH in relationship for Weibull location parameter	loc_{BB}	–	Observed	0.872	0.505
Slope of relative height for Weibull location parameter	loc_{Brh}	–	Observed	0.023	−0.626
Slope of age in relationship for Weibull location parameter	loc_{Bt}	–	Observed	0	0
Slope of competition for Weibull location parameter	loc_{BC}	–	Observed	−0.106	0.046
ws distributions					
Constant for Weibull scale parameter of ws dist.	sc_{w0}		Observed	0.090	0.022
Slope of DBH in relationship for Weibull scale parameter	sc_{wB}		Observed	2.084	2.605
Slope of relative height for Weibull scale parameter	sc_{wrh}		Observed	0	−1.815
Slope of age in relationship for Weibull scale parameter	sc_{wt}		Observed	0.271	0.321
Slope of competition for Weibull scale parameter	sc_{wC}		Observed	−0.122	0.090
Constant in the relationship for Weibull shape parameter	sh_{w0}		Observed	1.134	0.646
Slope of DBH in relationship for Weibull shape parameter	sh_{wB}		Observed	0	0.269
Slope of relative height for Weibull shape parameter	sh_{wrh}		Observed	0.945	1.740
Slope of age in relationship for Weibull shape parameter	sh_{wt}		Observed	0	0
Slope of competition for Weibull shape parameter	sh_{wC}		Observed	0.122	−0.143
Constant in the relationship for Weibull location parameter	loc_{w0}		Observed	0.228	0.143
Slope of DBH in relationship for Weibull location parameter	loc_{wB}	–	Observed	2.204	1.028
Slope of relative height for Weibull location parameter	loc_{wrh}	–	Observed	0	−3.450
Slope of age in relationship for Weibull location parameter	loc_{wt}	–	Observed	−0.418	0.453
Slope of competition for Weibull location parameter	loc_{wC}	–	Observed	0	0.208
Conversion factors					
Intercept of net v. solar radiation relationship	Q_a	W/m^2	Default	−90	−90
Slope of net v. solar radiation relationship	Q_b	–	Default	0.8	0.8
Molecular weight of dry matter		gDM/mol	Default	24	24
Conversion of solar radiation to PAR		mol/MJ	Default	2.3	2.3

Calculation options
Apply 3PGpjs light model = no
Apply 3PGpjs water balance = no
Apply 3PGpjs Physmod = yes
Dbh and ws distribution type = provided

Table A2
Stand and site characteristics for the 26 sites sorted by the de Martonne aridity index. When a given characteristic varied between plots within a site, values for each plot are provided as *F. sylvatica* monoculture/*P. sylvestris* monoculture/Mixture. Site index is a site productivity index calculated as the height of the 100 largest-diameter trees per ha at age 50 years (using data from monocultures only).

ID	Site code	Longitude	Latitude	Altitude	Aspect (°)	Slope (°)	Mean annual temperature (°C)	Mean annual precipitation (mm)	Substrate	de Martonne index	Site index (m)	Date leaves begin absorbing PAR	Date leaves stop absorbing PAR
Ger_7	1061	13°36′58″/57″/54″	52°04′43″/43″/45″	76/68/76	0	0	8.6	520	Sandy	28	16.9/13.1	05/05/2013	15/11/2013
Pol_1	1035	14°36′18″	53°20′7″	60	0	0	9.2	556	Loamy sand and sand	29	27.3/26.9	30/04/2013	31/10/2013
Ger_6	1070	12°44′08″	48°11′12″	40	0	0	8	560	Slightly loamy sand	31.1	15.8/12.8	30/04/2013	15/10/2013
Ger_5	1034	08°10′49″	48°59′12″	370	0	3	10	675	Slightly loamy sand	33.4	24.4/23.6	30/04/2013	22/10/2013
Cze_1	1049	16°36′10″/7″/9″	49°18′14″/15″/14″	435/445/440	45	5–15/0–10/5–10	7.5	620	Cambisol mezotrofic	35.4	23.8/23.0	25/04/2013	22/10/2013
Pol_4	1044	20°24′33″/23′38″/13′46″	50°0′51″/2′53″/1′28″	210/205/210	0	0/0/4	8.2	650	Slightly loamy sand	35.7	15.8/21.3	07/05/2013	15/11/2013
Pol_5	1045	20°14′21″/20′50″/19′37″	50°1′30″/2′31″/1′36″	210/210/220	0	0	8.2	650	Loamy sand	35.7	25.8/24.5	07/05/2013	15/11/2013
Ger_3	1032	10°58′13″	49°53′12″	250	30	2	8	650	Loamy sand	36.1	24.4/25.2	22/04/2013	31/10/2013
Pol_2	1036	19°54′42″	53°48′19″	136	0	0	7.9	666	Slightly loamy sand	37.2	19.1/25.5	07/05/2013	31/10/2013
Pol_3	1037	20°41′09″	50°59′28″	383	275	2	7.8	662	Sandstone loamy sand and loam	37.2	22.6/20.5	30/04/2013	31/10/2013
Ger_1	1033	11°14′12″	48°34′58″	430	45	1	8.5	700	Slightly loamy sand	37.8	27.6/22.7	30/04/2013	22/10/2013
Ger_2	1031	9°3′54″	50°6′49″	250	20	0	9	720	Slightly loamy sand	37.9	23.1/25.7	15/04/2013	22/10/2013
Swe_1	1054	13°35′29″/11″/35″	56°8′50″/8′59″/9′12″m	130/120/110	270/270/125	10/11/2017	8	700	Loamy sand	38.9	13.3/21.0	22/04/2013	15/10/2013
Bel_1	1063	04°19′30″	50°45′06″	120	0	0	10.5	852	Loam	41.6	12.0/10.9	01/05/2013	31/10/2013
Net_1	1043	6°1′22″/28″/20″	52°25′40″/41″/41″	34/34/35	90/0/45	3.4/0/2.3	9.7	825	Coarse sand	41.9	17.4/17.9	01/05/2013	01/11/2013
Lit_1	1051	22°24′24″	55°04′47.30″	20	0	0	6.5	750	Sand and slightly loamy sand	45.5	22.3/19.5	05/05/2013	15/10/2013
Sp_1	1042	3°10′33″W/0′W/19′W	42°6′10″/5′48″/5′57″	1252/1339/1289	45/0/315	43/53/45	8.9	860	Sandy loam	45.5	24.8/20.9	15/05/2013	15/11/2013
Bul_1	1047	23°21′02″	41°53′44″	1180	360/360/330	20/20/15	6	750	Loamy sand	46.9	25.9/25.1	31/05/2013	01/11/2013
Swe_2	1053	14°11′49″/51″/46″	55°42′41″/42″/33″	20/25/30	180/180/0	15/05/2004	7	800	Sandy till	47.1	22.0/22.0	22/04/2013	15/10/2013
Fran_1	1040	7°29′14″	48°58′42″	275	315	28/38/35	9.7	948	Sandstone sandy soil	48.1	22.2/23.0	15/05/2013	15/11/2013
BHe_1	1059	18°29′56″	44°13′35″	627	225	25	9.5	939	Loam to sandy clay	48.2	13.2/16.1	30/04/2013	01/11/2013
Lit_2	1052	21°32′23″	55°27′02″	25	0	0	6.5	800	Sand and slightly loamy sand	48.5	13.6/22.9	05/05/2013	15/10/2013
Ita_2	1062	07°03′53″	44°54′12″	1250	315	25	7.9	938	Sandy loam	52.4	19.9/16.9	30/04/2013	01/11/2013
Ser_1	1056	19°37′30″	43°42′17″	1090	0	20	7.7	1020	Loam	57.6	11.7/14.7	30/04/2013	01/11/2013
Sp_2	1041	2°16′0″/16′26″/15′44″	42°10′15″/46″/18″	1065/1209/1074	45/315/45	39.8/24.4/26.6	8	1100	Loam slightly clay	61.1	24.3/9.5	15/05/2013	15/11/2013
Bel_2	1057	05°27′00″	50°01′48″	530	180	8	7.5	1175	Stony loam	67.1	13.2/17.3	01/05/2013	15/10/2013

Appendix B

Height, live-crown length and crown diameter equations (Eqs. (3)–(5)).

The height of each species was a function of diameter, but for *F. sylvatica*, the competition index was also a significant predictor (Table B1). The crown diameter of *P. sylvestris* was also related to the competition index, in addition to stem diameter, while the crown diameter of *F. sylvatica* was only significantly related by stem diameter. Live-crown lengths of both species were related to the competition index and *P. sylvestris* crown lengths were also related to their relative height (Table B1).

Fig. B1. The effects of mean diameter (*B*), relative height (*rh*), age and competition index (*CI*; Eq. (6)) on the diameter distributions of *F. sylvatica* and *P. sylvestris*. These plots are created using Eqs. (B1)–(B6) and by varying only one of the independent variables at a time, and holding all others at their mean values for the given species.
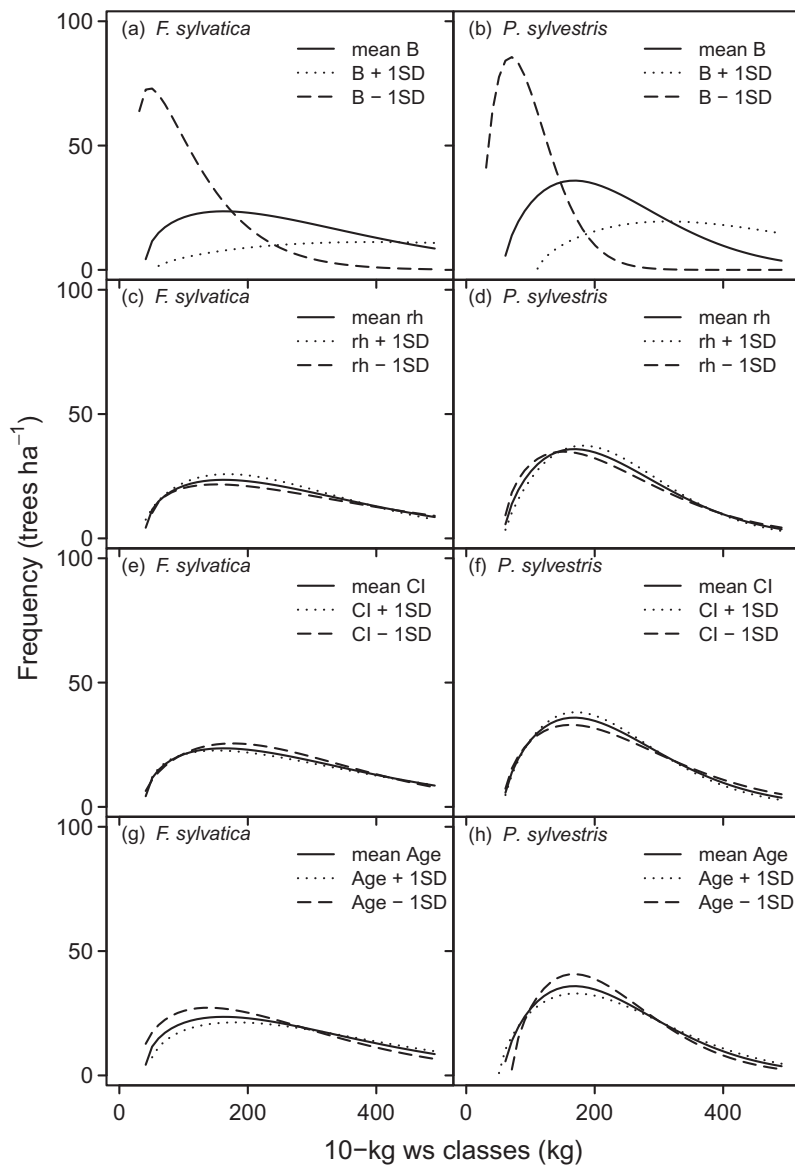
Fig. B2. The effects of mean diameter (*B*), relative height (*rh*), age and competition index (*CI*; Eq. (6)) on the stem mass (w_s) distributions of *F. sylvatica* and *P. sylvestris*. These plots are created using Eqs. (B1)–(B6) and by varying only one of the independent variables at a time, and holding all others at their mean values for the given species.

B.1. Diameter and stem mass distributions

3-PG$_{mix}$ uses diameter or stem mass distributions for two main purposes. One is to correct for the bias that can result from Jensen's Inequality when allometric equations are used to calculate means of variables (e.g. mean diameter) instead of individual tree values; the mean of a function is not the same as the function of the mean (Duursma and Robinson, 2003). The second use of the distributions, is to provide the user with the option to thin the stand and to obtain outputs for a given number of crop trees (e.g. the largest 100 trees per ha) or the parameters of the Weibull distributions themselves (Forrester and Tang, 2016).

In this study, the distributions were described using 3-parameter Weibull distributions (Forrester and Tang, 2016). The scale, shape and location parameters of the Weibull distributions were calculated using the percentile method, as described by Nanang (1998) using the data collected from the triplets. The w_s was calculated using generalised biomass equations from Forrester et al. (2017b). In the mixed-species plots, the size distributions of a given species were converted to equivalent monospecific size distributions by dividing the trees per ha of each size class (for the given species) by the mixing proportion for that species in terms of basal area.

The scale, shape and location parameters were then fitted to Eqs. (B1)–(B6) where they are described as functions of mean diameter (*B*, cm), relative height (*rh*, height of the target species divided by the mean height of all species in the plot), age (*A*, years) and competition, which as
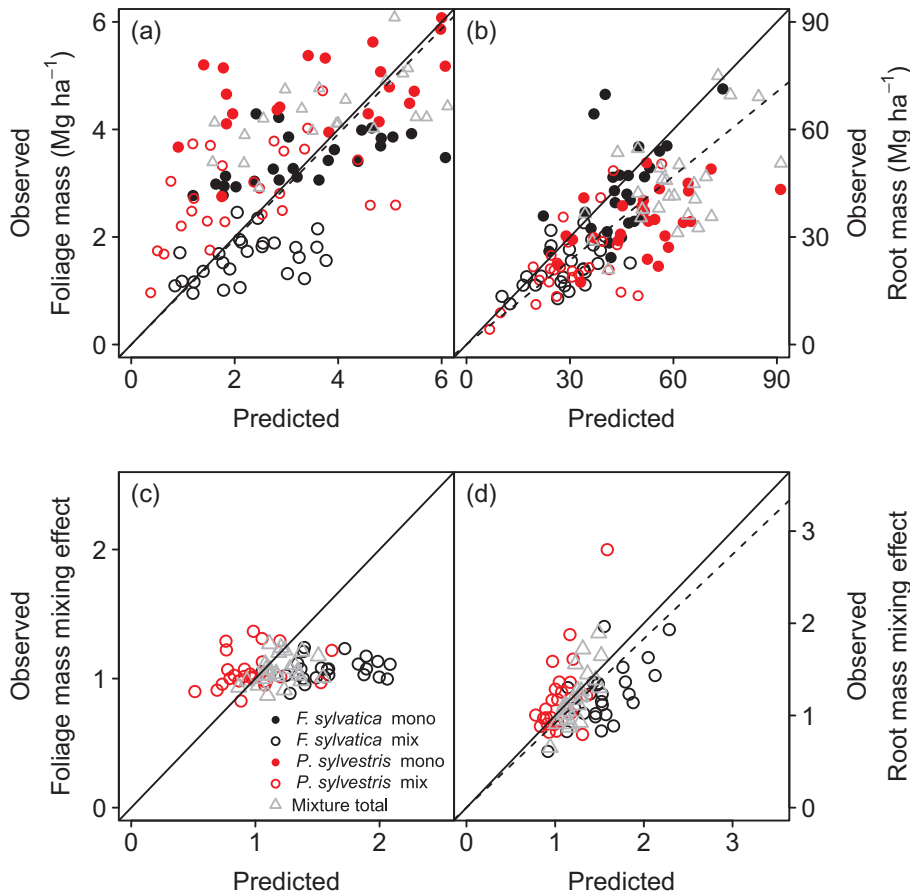
Fig. B3. Comparison of observed and predicted foliage mass (W_F, a), root mass (W_R, b) and mixing effects on foliage mass (c) and root mass (d), all for the end of 2012. The solid lines are 1:1 lines and the dashed lines are lines fitted to the data that pass through the origin. For each species-treatment combination n = 26.

calculated using Eq. (6). Eqs. (B1)–(B6) were fitted as mixed models with site as the random variable using the *nlme* package for fitting the mixed models (Harrison et al., 2009) with R 3.2.1 (R Core Team, 2015).

$$\ln(loc_B) = loc_{B0} + loc_{BB} \times \ln(B) + loc_{Brh} \times \ln(rh) + loc_{Bt} \times \ln(Age) + loc_{BC} \times \ln(C) \tag{B1}$$

$$ln(sc_B) = sc_{B0} + sc_{BB} \times \ln(B) + sc_{Brh} \times \ln(rh) + sc_{Bt} \times \ln(Age) + sc_{BC} \times \ln(C) \tag{B2}$$

$$ln(sh_B) = sh_{B0} + sh_{BB} \times \ln(B) + sh_{Brh} \times \ln(rh) + sh_{Bt} \times \ln(Age) + sh_{BC} \times \ln(C) \tag{B3}$$

$$ln(loc_w) = loc_{w0} + loc_{wB} \times \ln(B) + loc_{wrh} \times \ln(rh) + loc_{wt} \times \ln(Age) + loc_{wC} \times \ln(C) \tag{B4}$$

$$ln(sc_w) = sc_{w0} + sc_{wB} \times \ln(B) + sc_{wrh} \times \ln(rh) + sc_{wt} \times \ln(Age) + sc_{wC} \times \ln(C) \tag{B5}$$

$$ln(sh_w) = sh_{w0} + sh_{wB} \times \ln(B) + sh_{wrh} \times \ln(rh) + sh_{wt} \times \ln(Age) + sh_{wC} \times \ln(C) \tag{B6}$$

where loc_{Bx}, sc_{Bx} and sh_{Bx} are fitted parameters for the B distributions, and loc_{wx}, sc_{wx} and sh_{wx} are fitted parameters for the w_s distributions.

Eqs. (B1)–(B6) differ from the equations in the original 3-PG$_{mix}$ described by Forrester and Tang (2016) because ln-transformations were found to be necessary to reduce heteroscedasticity and to linearize relationships. The parameter estimates for Eqs. (B1)–(B6) are shown in Table B2 and the distributions are shown in Figs. B1 and B2.

Mean stand diameter, for the given species, was the strongest predictor of the shape of diameter distributions and also of the w_S distributions (Figs. B1 and B2; Table B2). For both species, there were also small, but significant, effects of the competition index, relative height and age, with the exception of age in the *P. sylvestris* diameter distribution equations.

Table B1
Parameter estimates (with their standard errors) and random effects for Eqs. (3)–(5) that describe the (ln-transformed) height (m), crown diameter (m) and live-crown length (m) of *P. sylvestris* and *F. sylvatica*.

	F. sylvatica	*P. sylvestris*
Stem height		
$\ln(a_H)$	−0.002 (0.215)	1.519 (0.054)
n_{HB}	0.538 (0.008)	0.474 (0.011)
n_{HC}	0.45 (0.071)	
Correction factor	1.0095	1.0047
n	2324	1778
ε_{ij}	0.158	0.118
Standard deviation (sd) for random effects (sd_i /sd_{ij})		
Estimate	0.137/0.161	0.177/0.088
Lower	0.083/0.122	0.125/0.065
Upper	0.228/0.213	0.252/0.118
Live-crown length		
$\ln(a_{HL})$	1.802 (0.091)	0.753 (0.322)
n_{HLB}	0.189 (0.024)	0.563 (0.036)
n_{HLC}	0.655 (0.037)	−0.266 (0.101)
n_{HLrh}		0.678 (0.055)
Correction factor	1.0344	1.0304
n	2314	1778
ε_{ij}	0.286	0.278
Standard deviation (sd) for random effects (sd_i/sd_{ij})		
Estimate	0.226/0.146	0.164/0.132
Lower	0.156/0.107	0.102/0.093
Upper	0.328/0.198	0.264/0.188
Crown diameter		
$\ln(a_K)$	−0.093 (0.059)	0.283 (0.28)
n_{KB}	0.581 (0.015)	0.554 (0.022)
n_{KH}		
n_{KC}		−0.277 (0.091)
Correction factor	1.0303	1.0376
n	2108	1571
ε_{ij}	0.279	0.283
Standard deviation (sd) for random effects (sd_i /sd_{ij})		
Estimate	0.125/0.202	0.128/0.104
Lower	0.056/0.148	0.08/0.071
Upper	0.277/0.277	0.205/0.154

n = the sample number; ε_{ij} = the residual variance, correction factor is as described in the text (Snowden, 1991).

Table B2

Parameter estimates (with their standard errors) and random effects for Eqs. (B1)–(B6) that describe the (ln-transformed) parameters of Weibull distributions, for diameter and stem mass, of *P. sylvestris* and *F. sylvatica*. The parameters loc_{Bx}, sc_{Bx} and sh_{Bx} are fitted parameters for the diameter distributions and loc_{wx}, sc_{wx} and sh_{wx} are fitted parameters for the stem mass distributions.

Diameter distribution			Stem mass distribution		
	F. sylvatica	*P. sylvestris*		*F. sylvatica*	*P. sylvestris*
Scale parameter					
$\ln(sc_{B0})$	−1.638 (0.202)	−1.28 (0.234)	$\ln(sc_{w0})$	−3.812 (0.229)	−2.408 (0.306)
sc_{BB}	1.225 (0.031)	1.152 (0.06)	sc_{wB}	2.605 (0.042)	2.084 (0.052)
sc_{Brh}			sc_{wrh}	−1.815 (0.184)	
sc_{Bt}	0.128 (0.052)		sc_{wt}	0.321 (0.061)	0.271 (0.086)
sc_{BC}		0.054 (0.024)	sc_{wC}	0.09 (0.021)	−0.122 (0.021)
n	635	631	n	635	607
ε_i	0.089	0.193	ε_i	0.113	0.144
Standard deviation for random effects			*Standard deviation for random effects*		
Estimate	0.184	0.227	Estimate	0.147	0.213
Lower	0.139	0.227	Lower	0.107	0.16
Upper	0.244	0.404	Upper	0.201	0.284
Shape parameter					
$\ln(sh_{B0})$	−0.238 (0.179)	0.206 (0.115)	$\ln(sh_{w0})$	−0.437 (0.207)	0.126 (0.112)
sh_{BB}	0.316 (0.059)		sh_{wB}	0.269 (0.068)	
sh_{Brh}	1.614 (0.291)	1.189 (0.193)	sh_{wrh}	1.74 (0.346)	0.945 (0.188)
sh_{Bt}			sh_{wt}		
sh_{BC}	−0.117 (0.032)	0.214 (0.04)	sh_{wC}	−0.143 (0.038)	0.122 (0.04)
n	635	631	n	635	607
ε_i	0.183	0.258	ε_i	0.221	0.25
Standard deviation for random effects			*Standard deviation for random effects*		
Estimate	0.156	0.267	Estimate	0.161	0.251
Lower	0.116	0.2	Lower	0.119	0.188
Upper	0.211	0.357	Upper	0.217	0.335
Location parameter					
$\ln(loc_{B0})$	0.492 (0.1)	−0.013 (0.225)	$\ln(loc_{w0})$	−1.947 (0.543)	−1.479 (0.821)
loc_{BB}	0.505 (0.032)	0.872 (0.061)	loc_{wB}	1.028 (0.092)	2.204 (0.113)
loc_{Brh}	−0.626 (0.141)	0.023 (0.15)	loc_{wrh}	−3.50 (0.392)	
loc_{Bt}			loc_{wt}	0.453 (0.141)	−0.419 (0.21)
loc_{BC}	0.046 (0.016)	−0.106 (0.03)	loc_{wC}	0.208 (0.045)	
n	635	631	n	635	607
ε_i	0.087	0.188	ε_i	0.238	0.381
Standard deviation for random effects			*Standard deviation for random effects*		
Estimate	0.179	0.27	Estimate	0.449	0.593
Lower	0.136	0.203	Lower	0.337	0.444
Upper	0.238	0.359	Upper	0.598	0.792

n = the sample number; ε_i = the residual variance.

References

Alcock, M.R., Morton, A.J., 1981. The sulphur content and pH of rainfall and throughfall under pine and birch. J. Appl. Ecol. 18, 835–839.

Almeida, A.C., Siggins, A., Batista, T.R., Beadle, C., Fonseca, S., Loos, R., 2010. Mapping the effect of spatial and temporal variation in climate and soils on *Eucalyptus* plantation production with 3-PG, a process-based growth model. For. Ecol. Manage. 259, 1730–1740.

Almeida, A.C.d., Landsberg, J.J., Sands, P.J, 2004. Parameterisation of 3-PG model for fast-growing *Eucalyptus grandis* plantations. For. Ecol. Manage. 193, 179–195.

Augusto, L., Ranger, J., Binkley, D., Rothe, A., 2002. Impact of several common tree species of European temperate forests on soil fertility. Ann. For. Sci 59, 233–253.

Barbaroux, C., 2002. Analyse et modélisation des flux de carbone de peuplements forestiers pour la compréhension de la croissance de deux espèces feuillues Quercus petraea et Fagus sylvatica. PhD thesis. University of Paris-Sud, Orsay, France, p. 178.

Barbier, S., Balandier, P., Gosselin, F., 2009. Influence of several tree traits on rainfall partitioning in temperate and boreal forests: a review. Ann. For. Sci. 66, 602.

Bauhus, J., Forrester, D.I., Gardiner, B., Jactel, H., Vallejo, R., Pretzsch, H., 2017a. Ecological stability of mixed-species forests. In: Pretzsch, H., Forrester, D.I., Bauhus, J. (Eds.), Mixed-Species Forests, Ecology and Management. Springer-Verlag, Berlin Heidelberg, pp. 339–384.

Bauhus, J., Forrester, D.I., Pretzsch, H., Felton, A., Pyttel, P., Benneter, A., 2017b. Silvicultural options for mixed-species stands. In: Pretzsch, H., Forrester, D.I., Bauhus, J. (Eds.), Mixed-Species Forests, Ecology and Management. Springer-Verlag, Berlin Heidelberg, pp. 435–503.

Bösch, B., 2003. Neue Schätzhilfen für Wuchsleistungen der Hauptbaumarten (New guide curves for the assessment of the growth potential of the main tree species in Baden-Wuerttemberg). Forstliche Versuchs- und Forschungsanstalt Baden-Württemberg. 12 p.

Cape, J.N., Brown, A.H.F., Robertson, S.M.C., Howson, G., Paterson, I.S., 1991. Interspecies comparisons of throughfall and stemflow at three sites in northern Britain. For. Ecol. Manage. 46, 165–177.

Charbonnier, F., Maire, G.I., Dreyer, E., Casanoves, F., Christina, M., Dauzat, J., Eitel, J.U.H., Vaast, P., Vierling, L.A., Roupsard, O., 2013. Competition for light in heterogeneous canopies: Application of MAESTRA to a coffee (*Coffea arabica* L.) agroforestry system. Agric. For. Meteorol. 181, 152–169.

Cienciala, E., Cerny, M., Alptauer, J., Exnerova, Z., 2005. Biomass functions applicable to European beech. J. For. Sci. 51, 147–154.

Condés, S., Río, M.D., 2015. Climate modifies tree interactions in terms of basal area growth and mortality in monospecific and mixed *Fagus sylvatica* and *Pinus sylvestris* forests. Eur. J. Forest Res. 134, 1095–1108.

Condés, S., Río, M.D., Sterba, H., 2013. Mixing effect on volume growth of *Fagus sylvatica* and *Pinus sylvestris* is modulated by stand density. For. Ecol. Manage. 292, 86–95.

Condés, S., Vallet, P., Bielak, K., Bravo-Oviedo, A., Coll, L., Ducey, M.J., Pach, M., Pretzsch, H., Sterba, H., Vayreda, J., Río, M.D., 2017. Climate influences on the maximum size-density relationship in Scots pine (*Pinus sylvestris* L.) and European beech (*Fagus sylvatica* L.) stands. For. Ecol. Manage. 385, 295–307.

Dee, D.P., Uppala, S.M., Simmons, A.J., Berrisford, P., Poli, P., Kobayashi, S., Andrae, U., Balmaseda, M.A., Balsamo, G., Bauer, P., Bechtold, P., Beljaars, A.C.M., Berg, L.V.D., Bidlot, J., Bormann, N., Delsol, C., Dragani, R., Fuentes, M., Geer, A.J., Haimberger, L., Healy, S.B., Hersbach, H., Hólm, E.V., Isaksen, L., Kållberg, P., Köhler, M., Matricardi, M., McNally, A.P., Monge-Sanz, B.M., Morcrette, J.-J., Park, B.-K., Peubey, C., Rosnay, P.D., Tavolato, C., Thépaut, J.-N., Vitart, F., 2011. The ERA-Interim reanalysis: configuration and performance of the data assimilation system. Quart. J. R. Meteorol. Soc. 137, 553–597.

del Río, M., Pretzsch, H., Ruíz-Peinado, R., Ampoorter, E., Annighöfer, P., Barbeito, I., Bielak, K., Brazaitis, G., Coll, L., Drössler, L., Fabrika, M., Forrester, D.I., Heym, M., Hurt, V., Kurylyak, V., Löf, M., Lombardi, F., Madrickiene, E., Matović, B., Mohren, F., Motta, R., den Ouden, J., Pach, M., Ponette, Q., Schütze, G., Skrzyszewski, J., Sramek, V., Sterba, H., Stojanović, D., Svoboda, M., Zlatanov, T., Bravo-Oviedo, A., 2017. Species interactions increase the temporal stability of community productivity in *Pinus sylvestris-Fagus sylvatica* mixtures across Europe. J. Ecol. 105, 1032–1043.

del Río, M., Sterba, H., 2009. Comparing volume growth in pure and mixed stands of *Pinus sylvestris* and *Quercus pyrenaica*. Ann. For. Sci. 66, 502.

Duursma, R.A., Robinson, A.P., 2003. Bias in the mean tree model as a consequence of Jensen's inequality. For. Ecol. Manage. 186, 373–380.

Faliński, J.B., 1986. Vegetation dynamics in temperate lowland Primeval Forests. Junk Publishers, Dordrecht, Ecological Studies in Białowieża Forest. Dr W, pp. 537.

Felbermeier, B., Mosandl, R., 2014. Fagus sylvatica. Wiley-VCH Verlag, In, Enzyklopädie der Holzgewächse.

Forrester, D.I., 2014. The spatial and temporal dynamics of species interactions in mixed-species forests: From pattern to process. For. Ecol. Manage. 312, 282–292.

Forrester, D.I., Ammer, C., Annighöfer, P.J., Barbeito, I., Bielak, K., Bravo-Oviedo, A., Coll, L., Río, M.d., Drössler, L., Heym, M., Hurt, V., Löf, M., Ouden, J.d., Pach, M., Pereira, M.G., Plaga, B., Ponette, Q., Skrzyszewski, J., Sterba, H., Svoboda, M., Zlatanov, T., Pretzsch, H., in press. Effects of crown architecture and stand structure on light absorption in mixed and monospecific *Fagus sylvatica* and *Pinus sylvestris* forests along a productivity and climate gradient through Europe. J. Ecol. 10.1111/1365-2745.12803.

Forrester, D.I., Bauhus, J., 2016. A review of processes behind diversity - productivity relationships in forests. Curr. Forest Rep. 2, 45–61.

Forrester, D.I., Benneter, A., Bouriaud, O., Bauhus, J., 2017a. Diversity and competition influence tree allometry – developing allometric functions for mixed-species forests. J. Ecol. 105, 761–774.

Forrester, D.I., Guisasola, R., Tang, X., Albrecht, A.T., Dong, T.L., le Maire, G., 2014.

Using a stand-level model to predict light absorption in stands with vertically and horizontally heterogeneous canopies. For. Ecosyst. 1, 17.

Forrester, D.I., Kohnle, U., Albrecht, A.T., Bauhus, J., 2013. Complementarity in mixed-species stands of *Abies alba* and *Picea abies* varies with climate, site quality and stand density. For. Ecol. Manage. 304, 233–242.

Forrester, D.I., Pretzsch, H., 2015. Tamm Review: On the strength of evidence when comparing ecosystem functions of mixtures with monocultures. For. Ecol. Manage. 356, 41–53.

Forrester, D.I., Tachauer, I.H.H., Annighoefer, P., Barbeito, I., Pretzsch, H., Ruiz-Peinado, R., Stark, H., Vacchiano, G., Zlatanov, T., Chakraborty, T., Saha, S., Sileshi, G.W., 2017b. Generalized biomass and leaf area allometric equations for European tree species incorporating stand structure, tree age and climate. For. Ecol. Manage. 396, 160–175.

Forrester, D.I., Tang, X., 2016. Analysing the spatial and temporal dynamics of species interactions in mixed-species forests and the effects of stand density using the 3-PG model. Ecol. Model. 319, 233–254.

Garber, S.M., Maguire, D.A., 2004. Stand productivity and development in two mixed-species spacing trials in the Central Oregon Cascades. Forest Science 50, 92–105.

Gash, J.H.C., Stewart, J.B., 1977. The evaporation from Thetford Forest during 1975. J. Hydrol. 35, 385–396.

Gerrits, A.M.J., Pfister, L., Savenije, H.H.G., 2010. Spatial and temporal variability of canopy and forest floor interception in a beech forest. Hydrol. Process. 24, 3011–3025.

Gonzalez-Benecke, C.A., Jokela, E.J., Cropper Jr, W.P., Bracho, R., Leduc, D.J., 2014. Parameterization of the 3-PG model for *Pinus elliottii* stands using alternative methods to estimate fertility rating, biomass partitioning and canopy closure. For. Ecol. Manage. 327, 55–75.

Gonzalez-Benecke, C.A., Teskey, R.O., Martin, T.A., Jokela, E.J., Fox, T.R., Kane, M.B., Noormets, A., 2016. Regional validation and improved parameterization of the 3-PG model for *Pinus taeda* stands. For. Ecol. Manage. 361, 237–256.

Grimm, V., 1999. Ten years of individual-based modelling in ecology: what have we learned and what could we learn in the future? Ecol. Model. 115, 129–148.

Gryc, V., Vavrčík, H., Gomola, Š., 2008. Selected properties of European beech (*Fagus sylvatica* L.). J. For. Sci. 54, 418–425.

Härkönen, S., Pulkkinen, M., Duursma, R., Mäkelä, A., 2010. Estimating annual GPP, NPP and stem growth in Finland using summary models. For. Ecol. Manage. 259, 524–533.

Harrison, R.B., Terry, T.A., Licata, C.W., Flaming, B.L., Meade, R., Guerrini, I.A., Strahm, B.D., Xue, D., Lolley, M.R., Sidell, A.R., Wagoner, G.L., Briggs, D., Turnblom, E.C., 2009. Biomass and stand characteristics of a highly productive mixed Douglas-fir and western hemlock plantation in coastal Washington. West. J. Appl. Forest. 24, 180–186.

Heym, M., Ruíz-Peinado, R., del Río, M., Bielak, K., Forrester, D.I., Dirnberger, G., Barbeito, I., Brazaitis, G., Ruškytė, I., Coll, L., Fabrika, M., Drössler, L., Löf, M., Sterba, H., Hurt, V., Kurylyak, V., Lombardi, F., Stojanović, D., Ouden, J.d., Motta, R., Pach, M., Skrzyszewski, J., Ponette, Q., de Streel, G., Sramek, V., Čihák, T., Zlatanov, T.M., Avdagic, A., Ammer, C., Verheyen, K., Włodzimierz, B., Bravo-Oviedo, A., Pretzsch, H., 2017. Data from: EuMIXFOR empirical forest mensuration and ring width data from pure and mixed stands of Scots pine (Pinus sylvestris L.) and European beech (Fagus sylvatica L.) through Europe. Dryad Digital Repository. 10.5061/dryad.8v04m.

Heym, M., Ruíz-Peinado, R., del Río, M., Bielak, K., Forrester, D.I., Dirnberger, G., Barbeito, I., Brazaitis, G., Ruškytė, I., Coll, L., Fabrika, M., Drössler, L., Löf, M., Sterba, H., Hurt, V., Kurylyak, V., Lombardi, F., Stojanović, D., Ouden, J.d., Motta, R., Pach, M., Skrzyszewski, J., Ponette, Q., de Streel, G., Sramek, V., Čihák, T., Zlatanov, T.M., Avdagic, A., Ammer, C., Verheyen, K., Włodzimierz, B., Bravo-Oviedo, A., Pretzsch, H., in press. EuMIXFOR empirical forest mensuration and ring width data from pure and mixed stands of Scots pine (Pinus sylvestris L.) and European beech (Fagus sylvatica L.) through Europe. Ann. For. Sci.10.1007/s13595-017-0660-z.

Huber, M.O., Sterba, H., Bernhard, L., 2014. Site conditions and definition of compositional proportion modify mixture effects in *Picea abies – Abies alba* stands. Can. J. For. Res. 44, 1281–1291.

Hung, T.T., Almeida, A.C., Eyles, A., Mohammed, C., 2016. Predicting productivity of *Acacia* hybrid plantations for a range of climates and soils in Vietnam. For. Ecol. Manage. 367, 97–111.

Janssen, P.H.M., Heuberger, P.S.C., 1995. Calibration of process-oriented models. Ecol. Model. 83, 55–66.

Jonard, F., André, F., Ponette, Q., Vincke, C., Jonard, M., 2011. Sap flux density and stomatal conductance of European beech and common oak trees in pure and mixed stands during the summer drought of 2003. J. Hydrol. 409, 371–381.

Köcher, P., Gebauer, T., Horna, Viviana, Leuschner, C., 2009. Leaf water status and stem xylem flux in relation to soil drought in five temperate broad-leaved tree species with contrasting water use strategies. Ann. For. Sci. 66, 101.

Landsberg, J., Mäkelä, A., Sievänen, R., Kukkola, M., 2005. Analysis of biomass accumulation and stem size distributions over long periods in managed stands of *Pinus sylvestris* in Finland using the 3-PG model. Tree Physiol. 25, 781–792.

Landsberg, J., Sands, P., 2010. Physiological Ecology of Forest Production: Principles, Processes and Models. Elsevier, Amsterdam, pp. 352.

Landsberg, J.J., Waring, R.H., 1997. A generalised model of forest productivity using simplified concepts of radiation-use efficiency, carbon balance and partitioning. For. Ecol. Manage. 95, 209–228.

le Maire, G., Nouvellon, Y., Christina, M., Ponzoni, F.J., Gonçalves, J.L.M., Bouillet, J.-P., Laclau, J.-P., 2013. Tree and stand light use efficiencies over a full rotation of single- and mixed-species *Eucalyptus grandis* and *Acacia mangium* plantations. For. Ecol. Manage. 288, 31–42.

Lehtonen, A., Mäkipää, R., Heikkinen, J., Sievänen, R., Liski, J., 2004. Biomass expansion

factors (BEFs) for Scots pine, Norway spruce and birch according to stand age for boreal forests. For. Ecol. Manage. 188, 211–224.

Leuschner, C., Voß, S., Foetzki, A., Clases, Y., 2006. Variation in leaf area index and stand leaf mass of European beech across gradients of soil acidity and precipitation. Plant Ecol. 186, 247–258.

Loague, K., Green, R.E., 1991. Statistical and graphical methods for evaluating transport models: overview and application. J. Contam. Hydrol. 7, 51–73.

Mäkelä, A., Pulkkinen, M., Kolari, P., Lagergren, F., Berbigier, P., Lindroth, A., Loustau, D., Nikinmaa, E., Vesala, T., Hari, P., 2008. Developing an empirical model of stand GPP with the LUE approach: analysis of eddy covariance data at five contrasting conifer sites in Europe. Glob. Change Biol. 14, 92–108.

Martonne, E., 1926. Une Nouvelle Fonction Climatologique: L'Indice d'Aridite (A New Climatological Function: The Aridity Index). La Météorologie 2, 449–458.

McMurtrie, R.E., Gholz, H.L., Linder, S., Gower, S.T., 1994. Climatic factors controlling the productivity of pine stands: a model-based analysis. Ecol. Bull. 43, 173–188.

Medlyn, B.E., 2004. A MAESTRO Retrospective. In: Mencuccini, M., Moncrieff, J., McNaughton, K., Grace, J. (Eds.), Forests at the Land-Atmosphere Interface. CABI Publishing, Wallingford UK, pp. 105–122.

Mette, T., Albrecht, A., Ammer, C., Biber, P., Kohnle, U., Pretzsch, H., 2009. Evaluation of the forest growth simulator SILVA on dominant trees in mature mixed Silver fir-Norway spruce stands in South-West Germany. Ecol. Model. 220, 1670–1680.

Nanang, D.M., 1998. Suitability of the Normal, Log-normal and Weibull distributions for fitting diameter distributions of neem plantations in Northern Ghana. For. Ecol. Manage. 103, 1–7.

Nihlgård, B., 1970. Precipitation, its chemical composition and effect on soil water in a Beech and a Spruce forest in south Sweden. Oikos 21, 208–217.

Paul, K.I., Booth, T.H., Jovanovic, T., Sands, P.J., Morris, J.D., 2007. Calibration of the forest growth model 3-PG to eucalypt plantations growing in low rainfall regions of Australia. For. Ecol. Manage. 243, 237–247.

Pretzsch, H., 2005. Link between the self-thinning rules for herbaceous and woody plants. Scientia agriculturae Bohemica 36, 98–107.

Pretzsch, H., del Río, M., Ammer, C., Avdagic, A., Barbeito, I., Bielak, K., Brazaitis, G., Coll, L., Dirnberger, G., Drössler, L., Fabrika, M., Forrester, D.I., Godvod, K., Heym, M., Hurt, V., Kurylyak, V., Löf, M., Lombardi, F., Matović, B., Mohren, F., Motta, R., den Ouden, J., Pach, M., Ponette, Q., Schütze, G., Schweig, J., Skrzyszewski, J., Sramek, V., Sterba, H., Stojanović, D., Svoboda, M., Vanhellemont, M., Verheyen, K., Wellhausen, K., Zlatanov, T., Bravo-Oviedo, A., 2015a. Growth and yield of mixed versus pure stands of Scots pine (*Pinus sylvestris* L.) and European beech (*Fagus sylvatica* L.) analysed along a productivity gradient through Europe. Eur. J. Forest Res. 134, 927–947.

Pretzsch, H., Forrester, D.I., Rötzer, T., 2015b. Representation of species mixing in forest growth models. A review and perspective. Ecol. Modell. 313, 276–292.

R Core Team, 2015. R: A Language and Environment for Statistical Computing. R Foundation for Statistical Computing, Vienna, Austria. < http://www.R-project.org/ > .

R Core Team, 2016. R: A Language and Environment for Statistical Computing. R Foundation for Statistical Computing, Vienna, Austria. < http://www.R-project.org > .

Rehfeldt, G.E., Tchebakova, N.M., Parfenova, Y.I., Wykoff, W.R., Kuzmina, N.A., Milyutin, L.I., 2002. Intraspecific responses to climate in *Pinus sylvestris*. Glob. Change Biol. 8, 912–929.

Richards, A.E., Forrester, D.I., Bauhus, J., Scherer-Lorenzen, M., 2010. The influence of mixed tree plantations on the nutrition of individual species: a review. Tree Physiol. 30, 1192–1208.

Robson, T.M., Sánchez-Gómez, D., Cano, F.J., Aranda, I., 2012. Variation in functional leaf traits among beech provenances during a Spanish summer reflects the differences in their origin. Tree Genet. Genom. 8, 1111–1121.

Rutter, A.J., 1963. Studies in the water relations of *Pinus sylvestris* in plantation conditions. I. Measurements of rainfall and interception. J. Ecol. 51, 165–184.

Ryan, M.G., Binkley, D., Fownes, J.H., 1997. Age-Related Decline in Forest Productivity: Pattern and Process. Adv. Ecol. Res. 27, 213–262.

San-Miguel-Ayanz, J., de Rigo, D., Caudullo, G., Houston Durrant, T., Mauri, A., 2016. European Atlas of Forest Tree Species. Publication Office of the European Union, Luxembourg.

Adaptation of 3-PG to novel species: guidelines for data collection and parameter assignment. Technical Report No.141. CRC for Sustainable Production Forestry, 35 p.

Sands, P.J., Landsberg, J.J., 2002. Parameterisation of 3-PG for plantation grown *Eucalyptus globulus*. For. Ecol. Manage. 163, 273–292.

Skovsgaard, J.P., Nord-Larsen, T., 2012. Biomass, basic density and biomass expansion factor functions for European beech (*Fagus sylvatica* L.) in Denmark. Eur. J. For. Res. 131, 1035–1053.

Snowden, P., 1991. A ratio estimator for bias correction in logarithmic regressions. Can. J. For. Res. 21, 720–724.

Spathelf, P., Ammer, C., 2015. Forest management of Scots pine (*Pinus sylvestris* L.) in northern Germany – a brief review of the history and current trends. Forstarchiv 86, 59–66.

Staelens, J., Schrijver, A.D., Verheyen, K., Verhoest, N.E.C., 2006. Spatial variability and temporal stability of throughfall water under a dominant beech (*Fagus sylvatica* L.) tree in relationship to canopy cover. J. Hydrol. 330, 651–662.

Staelens, J., Schrijver, A.D., Verheyen, K., Verhoest, N.E.C., 2008. Rainfall partitioning into throughfall, stemflow, and interception within a single beech (*Fagus sylvatica* L.) canopy: influence of foliation, rain event characteristics, and meteorology. Hydrol. Process. 22, 33–45.

Van Nevel, L., 2015. Tree species effects on Cd and Zn mobility after afforestation of contaminated soils in the Campine region (northern Belgium).

Vanclay, J.K., Skovsgaard, J.P., 1997. Evaluating forest growth models. Ecol. Model. 98, 1–12.

Vande Walle, I., van Camp, N., Perrin, D., Lemeur, R., Verheyen, K., van Wesemael, B., Laitat, E., 2005. Growing stock-based assessment of the carbon stock in Belgian forest biomass. Ann. For. Sci. 62, 853–864.

Waring, R.H., Landsberg, J.J., Williams, M., 1998. Net primary production of forests: a constant fraction of gross primary production. Tree Physiol. 18, 129–134.

Weiskittel, A.R., Maguire, D.A., Monserud, R.A., Johnson, G.P., 2010. A hybrid model for intensively managed Douglas-fir plantations in the Pacific Northwest, USA. Eur. J. For. Res. 129, 325–338.

Xenakis, G., Ray, D., Mencuccini, M., 2008. Sensitivity and uncertainty analysis from a coupled 3-PG and soil organic matter decomposition model. Ecol. Model. 219, 1–16.

Yoda, K., Kira, T., Ogawa, H., Hozami, K., 1963. Self thinning in overcrowded pure stands under cultivated and natural conditions. J. Biol. Osaka City Univ. 14, 107–129.